





RESEARCH ARTICLE

Cooperative midcourse guidance law with target changing and communication topology switching

R. Zhang^{1,2,3}, Y. Fang^{1,2,3,4}, Z. Chen^{1,2,3}, H. Guo^{1,2,3,4} and W. Fu^{1,2,3,4}

¹Unmanned System Research Institute, Northwestern Polytechnical University, Xi'an, 710072, China

²National Key Laboratory of Unmanned Aerial Vehicle Technology, Northwestern Polytechnical University, Xi'an, 710072, China

³Integrated Research and Development Platform of Unmanned Aerial Vehicle Technology, Northwestern Polytechnical University, Xi'an, 710072, China

⁴Research Center for Unmanned System Strategy Development, Northwestern Polytechnical University, Xi'an, 710072, China

Corresponding author: Y. Fang; Email: ywfang@nwpu.edu.cn

Received: 26 January 2024; **Revised:** 19 July 2024; **Accepted:** 30 September 2024

Keywords: Cooperative midcourse guidance; Target changing; Communication topology switching; Virtual interception point; Consensus protocol

Abstract

This paper proposes a cooperative midcourse guidance law with target changing and topology switching for multiple interceptors intercepting targets in the case of target loss and communication topology switching. Firstly, a three-dimensional guidance model is established and a cooperative trajectory shaping guidance law is given. Secondly, the average position consistency protocol of virtual interception points is designed for communication topology switching, and the convergence of the average position of virtual interception points under communication topology switching is proved by Lyapunov stability theory. Then, in the case of the target changing, the target handover law and the handover phase guidance law are designed to ensure the acceleration smoothing, at last, the whole cooperative midcourse guidance law is given based on the combination of the above guidance laws. Finally, numerical simulation results show the effectiveness and the superiority of the proposed cooperative midcourse guidance law.

Nomenclature

a_i	acceleration of the i th interceptor in the inertial coordinate frame (m/s^2)
a_T	acceleration of the target in the inertial coordinate frame (m/s^2)
A	adjacency matrix of graph G
G	communication network topology between interceptors
L	Laplace matrix of the graph G
N	number of interceptors
P_i	position of the i th interceptor in the inertial coordinate frame (m)
\tilde{P}_{xi}	the virtual interception point (m)
\bar{P}_{xi}	position of the interceptor after the flight the time-to-go t_{goi} according to the current position and speed (m)
P_T	position of the target in the inertial coordinate frame (m)
\bar{P}_x	average position of virtual interception points of all interceptors (m)
P_{old}	position of the old target (m)
P_{new}	position of the new target (m)
$P_{virtual}$	virtual target position (m)
t_{go}	time-to-go of the interceptor (s)
t_{goi}	time-to-go of the i th interceptor (s)
V_i	velocity of the i th interceptor in the inertial coordinate frame (m/s)
V_T	velocity of the target in the inertial coordinate frame (m/s)
\tilde{V}_{xi}	error between the interceptor velocity and the target velocity at the end of midcourse guidance (m/s)

\bar{V}_{xi}	real-time velocity error between interceptor and target (m/s)
$V_{approach}$	approach speed of the virtual target approaching the new target (m/s)
V_e	relative velocity between the old target and the new target (m/s)
V_{virtul}	virtual target velocity (m/s)

Greek Symbol

α_{xi}	the coordination coefficient
λ	parameter of the target handover law
$\dot{\gamma}$	heading angular velocity (deg/s)
$\Delta\gamma_{max}$	maximum allowable heading error (deg)
η	the coefficients of the handover law
q_e	elevation angle of LOS (deg)
q_β	azimuth angle of LOS (deg)

1.0 Introduction

With the rapid development of artificial intelligence, unmanned systems, materials and other technologies in recent years, the performance of target manoeuvring, decision-making and stealth has been greatly improved. This brings significant challenges to the interception and strike missions of a single interceptor. To improve the interceptor hit probability, most scholars apply cluster technology to interceptors to perform coordinated interception and strike missions. Through information sharing and functional complementation, multiple interceptors achieve coordinated strikes on targets and perform missions that are difficult to complete with a single interceptor.

Over the past few decades, scholars have conducted extensive research on cooperative guidance laws. Depending on the characteristics of the target, cooperative guidance laws can be categorised into those designed for low-mobility (stationary, uniform-speed, low-speed ground/sea targets) and high-mobility (high-speed, high-overload aerial targets) targets.

In the case of cooperative guidance laws for low-mobility targets, for the salvo attack of anti-ship missiles, a new guidance problem with impact time constraint was investigated in Jeon et al. [1] Xu et al. [2] investigated a time cooperative guidance law for multiple UAVs with the same strike time. Zhang et al. [3] addressed the optimal decentralised three-dimensional cooperative guidance problem for multiple interceptors against a stationary target considering dynamically changing and directed communication topologies. To solve the problem of the three-dimensional (3D) cooperative guidance of multiple interceptors attacking a stationary target, two nonsingular distributed cooperative guidance strategies were proposed in Yang et al. [4] Zhai et al. [5] proposed an event-triggered distributed cooperative guidance law for multiple missiles to simultaneously attack a stationary target with consideration of autopilot lag and unknown disturbances. An impact angle, speed and acceleration control guidance (IASAG) law against the stationary target was designed in Chen et al. [6], which was critical for the effectiveness of the air-to-surface guided weapons.

Regarding cooperative guidance laws for high-mobility targets, for the three-dimension terminal guidance problem of multiple cooperatively intercepting a manoeuvring target, Song et al. [7] investigated a novel finite-time cooperative guidance law with impact angle constraints. Kumar et al. [8] proposed a new approach to control the interception time for intercepting manoeuvring targets, using deviated pursuit. Aiming at the problem of multi-missile cooperative interception of manoeuvring targets, based on the time-to-go, the two different cooperative guidance laws were designed in Ma et al. [9] To address the issue of intercepting maneuvering targets at a specific time, a polynomial guidance method for impact-time control was proposed in Li et al. [10] In order to improve the multiple-missile cooperative attack capability and penetration capability, You et al. [11] investigated two three-dimensional impact-angle-constrained cooperative guidance strategies against manoeuvring target for controllable thrust missiles. Tao et al. [12] proposed an optimal 3-D spatial-temporal cooperative guidance (STCG) law for intercepting a manoeuvring target with impact angle and time constraints. Zhang et al. [13] designed finite-time distributed state estimation algorithm and cooperative guidance law for high manoeuvring target salvo attack.

From the above, it can be seen that currently, whether the target is low-mobility or high-mobility, the design of guidance laws focuses on the terminal guidance stage. Moreover, the related theories are relatively mature and can be extended to the midcourse guidance stage for designing cooperative midcourse guidance laws.

During cooperative strike missions, factors such as position changes, sensor performance limitations, and signal interference can lead to unstable communication links between interceptors, resulting in changes to the communication topology and affecting mission efficiency. Therefore, scholars have conducted extensive research on the cooperative strike problem of interceptor formations under topology switching. The consensus problem in directed networks with arbitrary finite time-varying communication delays under both fixed topology and switching topologies was investigated in Sun et al. [14] By using non-smooth analysis and fixed time stability techniques, Ning et al. [15] proposed the distributed protocols to achieve the fixed time consensus over fixed and switching topology. For leader-following missiles to intercept a manoeuvring target with switching communication topologies, Zhao et al. [16] investigated the cooperative time-varying formation guidance (CTRG) problem. Based on an extended state observer (ESO), a cooperative guidance method for multiple flight vehicles (MFV) cooperative interception with switching topologies was proposed in Zhao et al. [17] To address the practical fixed-time average consensus problems of first-order nonlinear multi-agent systems with external disturbances under switching topologies, Sun et al. [18] proposed a dynamic event-triggered fixed-time consensus protocol. Currently, research on cooperative guidance laws concerning topology switching mainly focuses on the terminal guidance stage, and the related theories are quite mature. However, there is still a gap in the design research of cooperative midcourse guidance laws for topology switching. Therefore, it is necessary to extend these theories to the midcourse guidance stage to address the design of cooperative midcourse guidance laws when multiple interceptors dynamically change network communication topology based on operational requirements.

With the rapid development of military equipment, medium- to long-range interceptors have been widely deployed for strategic strike missions. For medium- to long-range interceptors, with attack ranges extending over hundreds of kilometers, relying solely on terminal guidance during flight makes hitting targets challenging. To enhance accuracy, guidance in the midcourse phase is crucial. The transition between midcourse and terminal guidance techniques is particularly important. Many scholars have conducted extensive research on this technology. Concurrently, cooperative guidance techniques studied above have also undergone extensive simulation and validation on medium- to long-range interceptors.

Currently, there are relatively few research achievements regarding cooperative midcourse guidance. By using earliest intercept geometry (EIG) concept and the optimal control theory for area air defense, Shin et al. [19] proposed a cooperative midcourse missile guidance law. To impose a desired impact angle against stationary targets, based on sliding-mode control, nonlinear robust guidance strategies were proposed in Kumar et al. [20] For multiple missiles to intercept a target under the condition of large detection errors, Wang et al. [21] designed a novel cooperative midcourse guidance scheme. For providing suitable initial conditions of successful terminal salvo attack, a novel finite-time cooperative midcourse guidance law with terminal handover constraints was investigated in Zhang et al. [22] By combining the traditional trajectory shaping guidance law and the cooperative parameter, Wu et al. [23] proposed a novel cooperative midcourse guidance law. By combining the cooperative term with a distributed consensus protocol including communication delay under the directed communication topology, a novel distributed cooperative midcourse guidance (DCMG) law with communication delay was designed in Wu et al. [24] The above considerations, in designing cooperative midcourse guidance laws, include factors such as detection errors, terminal switching constraints and communication delays. During the midcourse phase, interceptors are typically far from the target, allowing ample time to adjust target attacks based on current situations, thereby achieving the objective of targeting high-value targets. Therefore, researching cooperative midcourse guidance related to target switching in this phase is crucial in this paper.

In the midcourse and terminal guidance handover, to achieve the trajectory handover of composite guidance, Hou et al. [25] proposed the concept of introducing the trajectory handover section and

conducting the handover section guidance. Wang et al. [26] considered the problem of compound guidance about mid-long range air-to-air missile. To resolve the problem of handover between midcourse guidance and terminal guidance in the combined guidance, Li et al. [27] designed a programme. Aiming at the trajectory shift of medium- and long-range missile in the course of midcourse and terminal guidance handover, based on the idea of shifted-guidance, Zhang et al. [28] designed a new shifted-law. For the trajectory shift of intercept missile in the course of midcourse and terminal guidance handover, a new shifted law was designed in Liu et al. [29] to realise two-order smooth transition. For the problem of fixed target missile guidance with virtual handover point, based on the optimisation theory in Hilbert space, a global energy optimal guidance law with/without terminal angle constraint was proposed in Li et al. [30] For the problem of midcourse and terminal guidance transition, based on the analysis of the constraints of trajectory smooth transition, Liu et al. [31] proposed a simple but effective method to realise smooth transition by using a linear operator. The above content focuses on the design of midcourse-to-terminal guidance handover laws. Since this paper primarily studies the midcourse phase of interceptors, where target switching can be conducted based on the current situation, it is important to avoid abrupt changes in guidance laws due to target switching. To address this, a handover law for target information can be designed based on this concept, allowing a smooth transition from old target information to new target information.

According to the research and analysis, for a cluster of medium- and long-range interceptors performing interceptor strike missions, the cooperative guidance phase is divided into three phases, namely formation organisation, cooperative midcourse guidance and cooperative terminal guidance. In the cooperative midcourse guidance phase, according to the mission requirements, some interceptors give up the cooperative strike mission and perform other missions. The remaining interceptors adjust the network topology according to the current situation. When the target is found to have been destroyed, target changing is performed to attack another target with higher value.

Based on the above research, a cooperative midcourse guidance law with target changing and topology switching is investigated in this paper to solve the problem of target loss and communication topology switching in the case of multiple interceptors intercepting targets. Compared with the existing literatures, the main merits of this paper are concluded as follows:

- ① For the problem of communication topology switching, an average position consistency protocol for virtual interception points is proposed, and the convergence is proved by Lyapunov stability theory.
- ② The target handover law and handover phase guidance law in the cooperative midcourse phase are designed for the interceptor changing target from the old to the new one.
- ③ The whole cooperative midcourse guidance law including the handover law method between phases are proposed in the case of target changing and communication topology switching.

The remainder of this paper is organised as follows: Section 2 gives the problem formulation and introduces some preliminaries. In Section 3, the cooperative midcourse guidance law, target handover law and whole cooperative midcourse guidance law are given. In Section 4, simulation results illustrate the effectiveness of the proposed guidance law. Finally, Section 5 gives the conclusion.

2.0 Problem formulation and preliminaries

2.1 Guidance model

In the inertial coordinate frame, the kinematic equation of the i th interceptor can be expressed as

$$\begin{cases} \dot{\mathbf{P}}_i(t) = \mathbf{V}_i(t) \\ \dot{\mathbf{V}}_i(t) = \mathbf{a}_i(t) \end{cases} \quad i = 1, 2, \dots, N \quad (1)$$

where, $\mathbf{P}_i(t) = [x_i(t), y_i(t), z_i(t)]^T$, $\mathbf{V}_i(t) = [V_{xi}(t), V_{yi}(t), V_{zi}(t)]^T$, $\mathbf{a}_i(t) = [a_{xi}(t), a_{yi}(t), a_{zi}(t)]^T$ represent the position, the velocity, the acceleration of the i th interceptor in the inertial coordinate frame, respectively.

The kinematic equation of the target can be given as

$$\begin{cases} \dot{\mathbf{P}}_T(t) = \mathbf{V}_T(t) \\ \dot{\mathbf{V}}_T(t) = \mathbf{a}_T(t) \end{cases} \quad (2)$$

where, $\mathbf{P}_T(t) = [x_T(t), y_T(t), z_T(t)]^T$, $\mathbf{V}_T(t) = [V_{Tx}(t), V_{Ty}(t), V_{Tz}(t)]^T$, $\mathbf{a}_T(t) = [a_{Tx}(t), a_{Ty}(t), a_{Tz}(t)]^T$ represent the position, the velocity, the acceleration of the target in the inertial coordinate frame, respectively.

2.2 Cooperative trajectory shaping guidance law

Based on the zero-effect miss distance and the optimal theory, the trajectory shaping guidance law is given in the line-of-sight coordinate frame, which can be expressed as [32]

$$a_c(t) = \frac{4(\mathbf{x}_T(t) - \mathbf{x}(t) + (\mathbf{V}_T(t) - \mathbf{V}(t))t_{go})}{t_{go}^2} + \frac{2(\mathbf{x}_T(t) - \mathbf{x}(t) + \bar{\mathbf{V}}_f t_{go})}{t_{go}^2} + \mathbf{a}_T(t) \quad (3)$$

where, $\mathbf{x}_T(t) - \mathbf{x}(t)$ indicates the zero-effect miss distance; $\mathbf{V}_T(t)$ and $\mathbf{V}(t)$ represent the speed of target and interceptor, respectively; $\bar{\mathbf{V}}_f = \mathbf{V}_T(t_f) - \mathbf{V}(t_f)$; t_{go} denotes the time-to-go of the interceptor; $\mathbf{a}_T(t)$ presents the acceleration of the target.

According to the Ref. [23], for the problem of cooperative interception of maneuvering or stealth targets by medium- and long-range interceptors, the cooperative term is introduced to optimise and improve the traditional trajectory shaping guidance law Equation (3). A new cooperative midcourse guidance law is proposed to achieve the purpose of cooperative interception. The acceleration of the i th interceptor on the x -axis in the inertial coordinate frame can be given as

$$a_{xi}(t) = \frac{6(\tilde{P}_{xi}(t) - \bar{P}_{xi}(t))}{t_{goi}^2} + \frac{2(\bar{V}_{xi}(t_{mf}) - \bar{V}_{xi}(t))}{t_{goi}} + a_{Tx}(t) - \alpha_{xi}(\tilde{P}_{xi}(t) - \hat{P}_x(t)) \quad i = 1, 2, \dots, N \quad (4)$$

where, t_{goi} is the time-to-go of the i th interceptor; $\tilde{P}_{xi}(t)$ indicates the virtual interception point; $\bar{P}_{xi}(t)$ represents the position of the interceptor after the flight time-to-go t_{goi} , based on the current position and speed; $\bar{V}_{xi}(t_{mf})$ represents the error between the interceptor velocity and the target velocity at the end of midcourse guidance; $\bar{V}_{xi}(t)$ presents the real-time velocity error between interceptor and target; $\hat{P}_x(t)$ denotes the average position of virtual interception points of all interceptors; α_{xi} is the coordination coefficient; N is the number of interceptors. The expressions are given as follows

$$\tilde{P}_{xi}(t) = x_T(t) + V_{Tx}(t) t_{goi} \quad (5)$$

$$\bar{P}_{xi}(t) = x_i(t) + V_{xi}(t) t_{goi} \quad (6)$$

$$\bar{V}_{xi}(t) = V_{Tx}(t) - V_{xi}(t) \quad (7)$$

$$\bar{V}_{xi}(t_{mf}) = V_{Tx}(t_{mf}) - V_{xi}(t_{mf}) \quad (8)$$

$$\hat{P}_x(t) = (\sum_{i=1}^N \tilde{P}_{xi}(t)) / N = x_T(t) + V_{Tx}(t) \bar{t}_{go} \quad (9)$$

$$\bar{t}_{go} = \frac{1}{N} \sum_{i=1}^N t_{goi} \quad (10)$$

The acceleration of the interceptor on the x -axis is given above. The acceleration on the y -axis and the z -axis is the same as the x -axis principle. Do not elaborate here.

2.3 Graph theories

In the multiple interceptors cooperative midcourse guidance, the communication network topology between interceptors can be described by a graph $G = (v, \varepsilon, A)$, where $v = \{1, 2, \dots, N\}$ represents the set of nodes; $\varepsilon \subset v \times v = \{(i, j) : i, j \in v\}$ indicates edges between nodes. $A = [a_{ij}] \in \mathbf{R}^{N \times N}$ ($i, j = 1, 2, \dots, N$) denotes the adjacency matrix of graph G . Assume that the communication topology is undirected, we have $a_{ij} = a_{ji} = 1$ if there is communication between the interceptor nodes i and j , otherwise $a_{ij} = a_{ji} = 0$. The Laplacian matrix of graph G is defined as $L = [l_{ij}] \in \mathbf{R}^{N \times N}$, which can be expressed as

$$l_{ij} = \begin{cases} \sum_{j=1}^N a_{ij}, & i = j \\ -a_{ij}, & i \neq j \end{cases} \tag{11}$$

In this paper, the following assumptions are made:

Assumption 1. *The communication network of multiple interceptors is undirected.*

Assumption 2. *The interceptor autopilot has no time delay, and the handover time T is mainly related to the handover heading error, and the handover heading error is less than the maximum allowable heading error.*

2.4 Correlation definitions and lemmas

Definition 1. [33] *Consider the following nonlinear system*

$$\dot{\mathbf{x}} = f(\mathbf{x}, t), f(\mathbf{0}, t) = \mathbf{0}, \mathbf{x} \in \mathbf{R}^n \tag{12}$$

where, $\mathbf{x} \in U \subseteq \mathbf{R}^n$; $f : U \rightarrow \mathbf{R}^n$ is a continuous function from the domain U containing the origin $\mathbf{x} = \mathbf{0}$ to space \mathbf{R}^n . For any initial condition $\mathbf{x}(0) = \mathbf{x}_0 \in U_0 \subseteq U$, there exists $T \geq 0$ such that the following equation holds

$$\begin{cases} \lim_{t \rightarrow T(\mathbf{x}_0)} \mathbf{x}(t, \mathbf{0}, \mathbf{x}_0) = \mathbf{0} \\ \text{If } t > T(\mathbf{x}_0), \text{ then } \mathbf{x}(t, \mathbf{0}, \mathbf{x}_0) = \mathbf{0} \end{cases} \tag{13}$$

according to Equation (13), it is known that the state of the system converges to the origin $\mathbf{x} = \mathbf{0}$ in finite time. In the neighbourhood U , if the system origin $\mathbf{x} = \mathbf{0}$ is Lyapunov stable and converges to a neighbourhood of the system origin in finite time, then the system origin $\mathbf{x} = \mathbf{0}$ is called finite-time stable. When $U = \mathbf{R}^n$, the origin is called globally finite-time stable.

Lemma 1. [34] *For system (13), in the domain U , if there is a continuously differentiable and radially unbounded positive definite function $V(x)$ that satisfies*

$$\dot{V}(\mathbf{x}) \leq -\beta V^p(\mathbf{x}), \mathbf{x} \in U \tag{14}$$

where β is positive constant, and p satisfies $p \in (0, 1)$. According to Definition 1, system (13) is finite-time stable. The system state can converge to the equilibrium point in finite time and the convergence time satisfies

$$T \leq \frac{1}{\beta(1-p)} V^{1-p}(\mathbf{x}_0) \tag{15}$$

Lemma 2. [35] If the graph G is undirected and connected, then for any $\xi = [\xi_1, \xi_2, \dots, \xi_n]^T \in \mathbf{R}^n$, we have $\xi^T L \xi = (1/2) \sum_{i=1}^n \sum_{j=1}^n a_{ij} (\xi_i - \xi_j)^2$.

Lemma 3. [35] If $z_1, z_2, \dots, z_n \geq 0$ and $0 < \varepsilon < 1$, then

$$\left(\sum_{i=1}^n z_i \right)^\varepsilon \leq \sum_{i=1}^n z_i^\varepsilon \tag{16}$$

Lemma 4. [36] If the function $y = f(x)$ has $n + 1$ different nodes, which are x_0, x_1, \dots, x_n , the function value is $y_i = f(x_i)$, and the derivative value is $y'_i = f'(x_i)$. The polynomial $H(x)$ of at most $2n + 1$ degrees is required to satisfy

$$H(x_i) = y_i, H'(x_i) = y'_i \tag{17}$$

According to Hermite interpolation theory, then we have

$$H(x) = \sum_{i=0}^n [y_i h_i(x) + y'_i H_i(x)] \tag{18}$$

When $n = 1$, the following expressions hold

$$\begin{cases} h_0(x) = \left(1 + 2 \frac{x - x_0}{x_1 - x_0} \right) \left(\frac{x - x_1}{x_0 - x_1} \right)^2 \\ h_1(x) = \left(1 + 2 \frac{x - x_1}{x_0 - x_1} \right) \left(\frac{x - x_0}{x_1 - x_0} \right)^2 \\ H_0(x) = (x - x_0) \left(\frac{x - x_0}{x_1 - x_0} \right)^2 \\ H_1(x) = (x - x_1) \left(\frac{x - x_0}{x_1 - x_0} \right)^2 \end{cases} \tag{19}$$

Then, according to Equation (20), the polynomial $H(x)$ of two points can be expressed as

$$\begin{aligned} H(x) = & \left(1 + 2 \frac{x - x_0}{x_1 - x_0} \right) \left(\frac{x - x_1}{x_0 - x_1} \right)^2 y_0 + \left(1 + 2 \frac{x - x_1}{x_0 - x_1} \right) \left(\frac{x - x_0}{x_1 - x_0} \right)^2 y_1 \\ & + (x - x_0) \left(\frac{x - x_0}{x_1 - x_0} \right)^2 y'_0 + (x - x_1) \left(\frac{x - x_0}{x_1 - x_0} \right)^2 y'_1 \end{aligned} \tag{20}$$

3.0 Main results

3.1 Design of cooperative midcourse guidance law

3.1.1 Design of guidance law

For the case that the communication topology of multiple interceptors is undirected and connected, based on the finite-time theory, a cooperative guidance law with communication topology switching is designed as

$$\left\{ \begin{aligned}
 a_{xi}(t) &= \frac{6(\tilde{P}_{xi}(t) - \bar{P}_{xi}(t))}{t_{goi}^2} + \frac{2(\tilde{V}_{xi}(t_{mf}) - \bar{V}_{xi}(t))}{t_{goi}} + a_{Tx}(t) - \alpha_{xi}(\tilde{P}_{xi}(t) - \hat{P}_{xi}(t)) \\
 \dot{\hat{P}}_{xi}(t) &= \sum_{j=1}^{N_i} a_{ij}(t) \operatorname{sign}[\hat{P}_{xj}(t) - \hat{P}_{xi}(t)] \left| \hat{P}_{xj}(t) - \hat{P}_{xi}(t) \right|^{\alpha_{xij}} \\
 a_{yi}(t) &= \frac{6(\tilde{P}_{yi}(t) - \bar{P}_{yi}(t))}{t_{goi}^2} + \frac{2(\tilde{V}_{yi}(t_{mf}) - \bar{V}_{yi}(t))}{t_{goi}} + a_{Ty}(t) - \alpha_{yi}(\tilde{P}_{yi}(t) - \hat{P}_{yi}(t)) \\
 \dot{\hat{P}}_{yi}(t) &= \sum_{j=1}^{N_i} a_{ij}(t) \operatorname{sign}[\hat{P}_{yj}(t) - \hat{P}_{yi}(t)] \left| \hat{P}_{yj}(t) - \hat{P}_{yi}(t) \right|^{\alpha_{yij}} \\
 a_{zi}(t) &= \frac{6(\tilde{P}_{zi}(t) - \bar{P}_{zi}(t))}{t_{goi}^2} + \frac{2(\tilde{V}_{zi}(t_{mf}) - \bar{V}_{zi}(t))}{t_{goi}} + a_{Tz}(t) - \alpha_{zi}(\tilde{P}_{zi}(t) - \hat{P}_{zi}(t)) \\
 \dot{\hat{P}}_{zi}(t) &= \sum_{j=1}^{N_i} a_{ij}(t) \operatorname{sign}[\hat{P}_{zj}(t) - \hat{P}_{zi}(t)] \left| \hat{P}_{zj}(t) - \hat{P}_{zi}(t) \right|^{\alpha_{zij}}
 \end{aligned} \right. \tag{21}$$

where, $0 < \alpha_{xij} < 1$; $0 < \alpha_{yij} < 1$; $0 < \alpha_{zij} < 1$; $\alpha_{xij} = \alpha_{xji}$; $\alpha_{yij} = \alpha_{yji}$; $\alpha_{zij} = \alpha_{zji}$; N_i denotes the number of the i th interceptor and its neighbour interceptor.

3.1.2 Stability analysis

Because the mathematical model of the interceptor is similar in the three directions of x , y and z , only the acceleration stability analysis in the x direction is given, and the principle of the other two directions is the same, which is not repeated here.

In the whole network topology, the average value of the virtual interception points for all distributed structures can be expressed as

$$P_{xi}^*(t) = \frac{1}{n} \sum_{i=1}^n \hat{P}_{xi}(t) \tag{22}$$

Then, according to Equation (21), the consensus protocol sum of all interceptors can be given as

$$\sum_{i=1}^n \dot{\hat{P}}_{xi}(t) = \sum_{i=1}^n \sum_{j=1}^{N_i} a_{ij}(t) \operatorname{sign}[\hat{P}_{xj}(t) - \hat{P}_{xi}(t)] \left| \hat{P}_{xj}(t) - \hat{P}_{xi}(t) \right|^{\alpha_{xij}} = 0 \tag{23}$$

where, $a_{ij}(t)$ represents the communication topology relationship between interceptors, and the communication topology structure is undirected and time-varying; n is the total number of interceptors, with $n \geq N_i$.

Obviously, according to Equation (23), $\sum_{i=1}^n \hat{P}_{xi}(t)$ is a constant value, so we can obtain

$$\sum_{i=1}^n \hat{P}_{xi}(t) = \sum_{i=1}^n \hat{P}_{xi}(0) \tag{24}$$

Furthermore, according to Equation (22), we can get

$$\hat{P}_{xi}(t) = P_{xi}^*(t) + \Delta_{xi}(t) = \frac{1}{n} \sum_{i=1}^n \hat{P}_{xi}(t) + \Delta_{xi}(t) \tag{25}$$

where, $\Delta_{xi}(t)$ is the difference value between the average value of the virtual interception points of the i th distributed structure composed of the i th interceptor and the average value of the virtual interception points of all distributed structures. In order to enable the interceptors to reach the handover area almost simultaneously, it needs to meet $\Delta_{xi}(t) \rightarrow 0$.

Then, according to Equation (25), we have

$$\sum_{i=1}^n \Delta_{xi}(t) = \sum_{i=1}^n \hat{P}_{xi}(t) - \sum_{i=1}^n \left[\frac{1}{n} \sum_{i=1}^n \hat{P}_{xi}(t) \right] = 0 \tag{26}$$

Meanwhile, combining Equations (21) and (23), according to Equation (25), we take the derivate of $\hat{P}_{xi}(t)$ with respect to time t as

$$\begin{aligned} \dot{\hat{P}}_{xi}(t) &= \frac{1}{n} \sum_{i=1}^n \dot{\hat{P}}_{xi}(t) + \dot{\Delta}_{xi}(t) \\ &= \dot{\Delta}_{xi}(t) \\ &= \sum_{j=1}^{N_i} a_{ij}(t) \text{sign} \left[\hat{P}_{xj}(t) - \hat{P}_{xi}(t) \right] \left| \hat{P}_{xj}(t) - \hat{P}_{xi}(t) \right|^{\alpha_{xij}} \end{aligned} \tag{27}$$

According to Equation (27), the Lyapunov function is denoted as

$$V_{xi} = \frac{1}{2} \sum_{i=1}^n \Delta_{xi}(t) \Delta_{xi}(t) \tag{28}$$

We take the derivate of V_{xi} with respect to time t as

$$\dot{V}_{xi} = \sum_{i=1}^n \Delta_{xi}(t) \dot{\Delta}_{xi}(t) \tag{29}$$

Then, substituting Equation (27) into Equation (29), we can obtain

$$\begin{aligned} \dot{V}_{xi} &= \sum_{i=1}^n \Delta_{xi}(t) \dot{\Delta}_{xi}(t) \\ &= \sum_{i=1}^n \Delta_{xi}(t) \sum_{j=1}^{N_i} a_{ij}(t) \text{sign} \left[\hat{P}_{xj}(t) - \hat{P}_{xi}(t) \right] \left| \hat{P}_{xj}(t) - \hat{P}_{xi}(t) \right|^{\alpha_{xij}} \end{aligned} \tag{30}$$

Furthermore, substituting Equation (25) into Equation (30), we have

$$\begin{aligned} \dot{V}_{xi} &= \sum_{i=1}^n \Delta_{xi}(t) \sum_{j=1}^{N_i} \left(a_{ij}(t) \text{sign} \left[\frac{1}{n} \sum_{j=1}^n \hat{P}_{xj}(t) + \Delta_{xj}(t) - \frac{1}{n} \sum_{i=1}^n \hat{P}_{xi}(t) - \Delta_{xi}(t) \right] \right. \\ &\quad \left. \cdot \left| \frac{1}{n} \sum_{j=1}^n \hat{P}_{xj}(t) + \Delta_{xj}(t) - \frac{1}{n} \sum_{i=1}^n \hat{P}_{xi}(t) - \Delta_{xi}(t) \right|^{\alpha_{xij}} \right) \\ &= \sum_{i=1}^n \Delta_{xi}(t) \sum_{j=1}^{N_i} a_{ij}(t) \text{sign} \left[\Delta_{xj}(t) - \Delta_{xi}(t) \right] \left| \Delta_{xj}(t) - \Delta_{xi}(t) \right|^{\alpha_{xij}} \end{aligned} \tag{31}$$

Then, by using Equation (26), we can rewrite Equation (31) as

$$\begin{aligned}
 \dot{V}_{xi} &= \sum_{i=1}^n \Delta_{xi}(t) \sum_{j=1}^{N_i} a_{ij}(t) \operatorname{sign} [\Delta_{xj}(t) - \Delta_{xi}(t)] |\Delta_{xj}(t) - \Delta_{xi}(t)|^{\alpha_{xij}} \\
 &= \sum_{i=1}^n \frac{1}{2} (\Delta_{xi}(t) - \Delta_{xj}(t)) \sum_{j=1}^{N_i} a_{ij}(t) \operatorname{sign} [\Delta_{xj}(t) - \Delta_{xi}(t)] |\Delta_{xj}(t) - \Delta_{xi}(t)|^{\alpha_{xij}} \\
 &= -\frac{1}{2} \sum_{i=1}^n (\Delta_{xj}(t) - \Delta_{xi}(t)) \sum_{j=1}^{N_i} a_{ij}(t) \operatorname{sign} [\Delta_{xj}(t) - \Delta_{xi}(t)] |\Delta_{xj}(t) - \Delta_{xi}(t)|^{\alpha_{xij}} \quad (32) \\
 &= -\frac{1}{2} \sum_{i=1}^n \sum_{j=1}^{N_i} a_{ij}(t) |\Delta_{xj}(t) - \Delta_{xi}(t)| |\Delta_{xj}(t) - \Delta_{xi}(t)|^{\alpha_{xij}} \\
 &= -\frac{1}{2} \sum_{i=1}^n \sum_{j=1}^{N_i} a_{ij}(t) |\Delta_{xj}(t) - \Delta_{xi}(t)|^{\alpha_{xij}+1} < 0
 \end{aligned}$$

According to Equations (28) and (32), the system is globally asymptotically stable. Meanwhile, according to Lemma 3, Equation (32) is also rewritten as

$$\begin{aligned}
 \dot{V}_{xi} &= -\frac{1}{2} \sum_{i=1}^n \sum_{j=1}^{N_i} a_{ij}(t) |\Delta_{xj}(t) - \Delta_{xi}(t)|^{\alpha_{xij}+1} \\
 &= -\frac{1}{2} \sum_{i=1}^n \sum_{j=1}^{N_i} \left\{ a_{ij}^{\frac{2}{1+\alpha_{xij}}}(t) \left[(\Delta_{xj}(t) - \Delta_{xi}(t))^2 \right]^{\frac{\alpha_{xij}+1}{1+\alpha_{xij}}} \right\}^{\frac{1+\alpha_{xij}}{2}} \\
 &\leq -\frac{1}{2} \left\{ \sum_{i=1}^n \sum_{j=1}^{N_i} a_{ij}^{\frac{2}{1+\alpha_0}}(t) \left[(\Delta_{xj}(t) - \Delta_{xi}(t))^2 \right]^{\frac{\alpha_{xij}+1}{1+\alpha_0}} \right\}^{\frac{1+\alpha_0}{2}} \\
 &= -\frac{1}{2} \left\{ \frac{\Xi_1}{\Xi_2} \frac{\Xi_3}{V_{xi}} \right\}^{\frac{1+\alpha_0}{2}}
 \end{aligned} \quad (33)$$

Where

$$\begin{aligned}
 \alpha_0 &= \max_{i,j} \alpha_{ij} \\
 \Xi_1 &= \sum_{i=1}^n \sum_{j=1}^{N_i} a_{ij}^{\frac{2}{1+\alpha_0}}(t) \left[(\Delta_{xj}(t) - \Delta_{xi}(t))^2 \right]^{\frac{\alpha_{xij}+1}{1+\alpha_0}} \\
 \Xi_2 &= \sum_{i=1}^n \sum_{j=1}^{N_i} a_{ij}^{\frac{2}{1+\alpha_0}}(t) \left[(\Delta_{xj}(t) - \Delta_{xi}(t))^2 \right] \\
 \Xi_3 &= \sum_{i=1}^n \sum_{j=1}^{N_i} a_{ij}^{\frac{2}{1+\alpha_0}}(t) \left[(\Delta_{xj}(t) - \Delta_{xi}(t))^2 \right]
 \end{aligned} \quad (34)$$

Suppose $(i_0, j_0) = \operatorname{argmax} (\Delta_{xj}(t) - \Delta_{xi}(t))^2$, when $(\Delta_{xj}(t) - \Delta_{xi}(t))^2$ takes the maximum value, that is, there is (i, j) taking (i_0, j_0) . The term of Ξ_1 in Equation (34) can be rewritten as

$$\begin{aligned} \Xi_1 &= \sum_{i=1}^n \sum_{j=1}^{N_i} a_{ij} \frac{2}{1+\alpha_0} (t) \left[(\Delta_{x_j}(t) - \Delta_{x_i}(t))^2 \right]^{\frac{\alpha_{x_j}+1}{1+\alpha_0}} \\ &\geq a_{i_0j_0} \frac{2}{1+\alpha_0} (t) \left[(\Delta_{x_{j_0}}(t) - \Delta_{x_{i_0}}(t))^2 \right]^{\frac{\alpha_{x_{j_0}}+1}{1+\alpha_0}} \end{aligned} \tag{35}$$

The term of Ξ_2 in Equation (34) can be rewritten as

$$\begin{aligned} \Xi_2 &= \sum_{i=1}^n \sum_{j=1}^{N_i} a_{ij} \frac{2}{1+\alpha_0} (t) \left[(\Delta_{x_j}(t) - \Delta_{x_i}(t))^2 \right] \\ &\leq \sum_{i=1}^n \sum_{j=1}^{N_i} a_{ij} \frac{2}{1+\alpha_0} (t) \left[(\Delta_{x_{j_0}}(t) - \Delta_{x_{i_0}}(t))^2 \right] \end{aligned} \tag{36}$$

Therefore, combining Equation (35) with Equation (36), we have

$$\begin{aligned} \frac{\Xi_1}{\Xi_2} &= \frac{\sum_{i=1}^n \sum_{j=1}^{N_i} a_{ij} \frac{2}{1+\alpha_0} (t) \left[(\Delta_{x_j}(t) - \Delta_{x_i}(t))^2 \right]^{\frac{\alpha_{x_j}+1}{1+\alpha_0}}}{\sum_{i=1}^n \sum_{j=1}^{N_i} a_{ij} \frac{2}{1+\alpha_0} (t) \left[(\Delta_{x_j}(t) - \Delta_{x_i}(t))^2 \right]} \\ &\leq \frac{a_{i_0j_0} \frac{2}{1+\alpha_0} (t) \left[(\Delta_{x_{j_0}}(t) - \Delta_{x_{i_0}}(t))^2 \right]^{\frac{\alpha_{x_{j_0}}+1}{1+\alpha_0}}}{\sum_{i=1}^n \sum_{j=1}^{N_i} a_{ij} \frac{2}{1+\alpha_0} (t) \left[(\Delta_{x_{j_0}}(t) - \Delta_{x_{i_0}}(t))^2 \right]} \\ &= K_1 \end{aligned} \tag{37}$$

Then, according to Lemma 2, we can rewrite the term of Ξ_3 in Equation (34) as

$$\begin{aligned} \Xi_3 &= \sum_{i=1}^n \sum_{j=1}^{N_i} a_{ij} \frac{2}{1+\alpha_0} (t) \left[(\Delta_{x_j}(t) - \Delta_{x_i}(t))^2 \right] \\ &= 2\mathbf{\Delta}_x^T \mathbf{L}(\mathbf{G}) \mathbf{\Delta}_x \end{aligned} \tag{38}$$

where

$$\begin{aligned} \mathbf{G} &= \left[a_{ij} \frac{2}{1+\alpha_0} (t) \right] \in \mathbf{R}^{n \times n} \\ \mathbf{\Delta}_x &= [\Delta_{x_1}, \Delta_{x_2}, \dots, \Delta_{x_n}]^T \end{aligned} \tag{39}$$

Furthermore, according to Equation (38), we can obtain

$$\begin{aligned} \frac{\Xi_3}{V_{x_i}} &= \frac{2\mathbf{\Delta}_x^T \mathbf{L}(\mathbf{G}) \mathbf{\Delta}_x}{\frac{1}{2}\mathbf{\Delta}_x^T \mathbf{\Delta}_x} \\ &\geq 4\lambda_2[\mathbf{L}(\mathbf{G})] \\ &> 0 \end{aligned} \tag{40}$$

where $\lambda_2[\mathbf{L}(\mathbf{G})]$ is the second smallest eigenvalue of the Laplacian matrix of \mathbf{G} .

Then, combining Equation (37) with Equation (40), we can rewrite Equation (33) as

$$\begin{aligned} \dot{V}_{xi} &= -\frac{1}{2} \left\{ \frac{\Xi_1 \Xi_3}{\Xi_2 V_{xi}} V_{xi} \right\}^{\frac{1+\alpha_0}{2}} \\ &\leq -\frac{1}{2} \{K_1 4\lambda_2[\mathbf{L}(\mathbf{G})]\}^{\frac{1+\alpha_0}{2}} V_{xi}^{\frac{1+\alpha_0}{2}} \\ &= -2^{\alpha_0} \{K_1 \lambda_2[\mathbf{L}(\mathbf{G})]\}^{\frac{1+\alpha_0}{2}} V_{xi}^{\frac{1+\alpha_0}{2}} \end{aligned} \tag{41}$$

Define $K_2 = \min \{K_1 \lambda_2[\mathbf{L}(\mathbf{G})]\}$, Equation (41) can be rewritten as

$$\dot{V}_{xi} \leq -2^{\alpha_0} K_2^{\frac{1+\alpha_0}{2}} V_{xi}^{\frac{1+\alpha_0}{2}} \tag{42}$$

According to Equations (28) and (42) and Lemma 1, we have

$$\lim_{t \rightarrow T_1} \Delta_{xi}(t) = 0 \tag{43}$$

where

$$T_1 = \frac{2^{1-\alpha_0} V_{xi}(0)^{\frac{1-\alpha_0}{2}}}{K_2^{\frac{1+\alpha_0}{2}} (1 - \alpha_0)} > 0 \tag{44}$$

Hence, combining Equation (25) with Equation (43), it is easy to get that

$$\lim_{t \rightarrow T_1} (\hat{P}_{xi} - \hat{P}_{xj}) = 0 \tag{45}$$

In summary, when the communication topology between interceptors is undirected and the connected time satisfies Equation (44), Equation (45) can be held to achieve the purpose of cooperative interception.

3.2 Design of target handover law

For the target handover law, this paper uses the virtual target method to study. In actual flight, the interceptor changes target according to mission requirements. Based on the old target, the position error between the old target and the new target is gradually increased to form a virtual target. The virtual target gradually replaces the new target to achieve the smooth handover of the target.

3.2.1 Handover model

Assume that multiple interceptors have reselected new targets based on mission requirements. By comparing the positions of the old target and the new target, the relative position can be expressed as

$$\mathbf{P}_e(t) = \mathbf{P}_{new}(t) - \mathbf{P}_{old}(t) \tag{46}$$

where, \mathbf{P}_{old} denotes the position of the old target; \mathbf{P}_{new} represents the position of the new target.

We take the derivate of $\mathbf{P}_e(t)$ with respect to time t as

$$\dot{\mathbf{P}}_e(t) = \mathbf{V}_e(t) \tag{47}$$

where \mathbf{V}_e is the relative velocity between the old target and the new target.

3.2.2 Design of handover method

(a) Handover time

In flight, when the interceptor performs target changing and guidance law handover, the handover time T is unknown. Therefore, it is necessary to design a suitable handover time T to achieve the smooth handover of target and guidance law.

The heading angular velocity of the interceptor can be given as

$$\dot{\gamma} = \frac{a(t)}{V} \tag{48}$$

where, $a(t)$ is the acceleration of the interceptor; V represents the velocity of the interceptor.

Suppose the acceleration at the beginning of the handover is $a_1(t_0)$ and the acceleration at the end is $a_2(t_0 + T)$. The acceleration error for the handover phase is denoted as

$$\Delta a = a_2(t_0 + T) - a_1(t_0) \tag{49}$$

Integrating Equation (49), with integration time T , we have

$$\int_{t_0}^{t_0+T} \Delta a dt \approx 0.5T (a_2 - a_1) \tag{50}$$

Then, according to Equations (48) and (50), the heading error of the interceptor during the handover can be expressed as

$$\begin{aligned} \Delta \gamma_m &= \left| \int_{t_0}^{t_0+T} \Delta a dt \right| \\ &\approx \left| \frac{0.5T (a_2 - a_1)}{V} \right| \end{aligned} \tag{51}$$

Assume that the maximum allowable heading error is $\Delta \gamma_{\max}$. According to Equation (51), we can obtain

$$T \leq \frac{2\Delta \gamma_{\max} V}{|a_2 - a_1|} \tag{52}$$

By selecting the handover time T satisfying Equation (52), the successful handover of target and guidance law can be realised.

(b) Target handover law

When changing target, the virtual target gradually approaches the new target on the basis of the old target. To achieve the overlap between the virtual target and the new target, the following expression needs to be satisfied.

$$\int_0^T V_{\text{approach}}(t) = P_e(t) \tag{53}$$

where $V_{\text{approach}}(t)$ is the approach speed of the virtual target approaching the new target.

The virtual target position can be defined as

$$P_{\text{virtual}}(t) = P_{\text{old}}(t) + \lambda(t) P_e(t) \tag{54}$$

where $\lambda(t)$ is the parameter of the target handover law. The target handover law parameter $\lambda(t)$ is designed for two cases.

(a) Case 1: The relative distance between the old target and the new target is a constant value

In this case, $P_e(t)$ is a constant value. Suppose that the virtual target moves from the old target position to the new target position at a constant velocity, we have

$$V_{\text{approach}}(t) = \frac{P_e(t)}{T} = \text{const} \tag{55}$$

where T denotes the time required to complete the handover of target.

Then, by using Equation (55), the virtual target velocity is denoted as

$$\begin{aligned} V_{\text{virtual}}(t) &= V_{\text{old}}(t) + V_{\text{approach}}(t) \\ &= V_{\text{old}}(t) + \frac{P_e(t)}{T} \end{aligned} \tag{56}$$

Furthermore, integrating Equation (56), the virtual target position can be expressed as

$$\mathbf{P}_{virtual}(t) = \mathbf{P}_{old}(t) + \frac{t}{T} \mathbf{P}_e(t) \tag{57}$$

By comparing Equation (57) with Equation (54), we can get

$$\lambda(t) = \frac{t}{T}, t \in [0, T] \tag{58}$$

According to Equation (57), the virtual target overlaps with the new target at time T , the target changing is achieved.

(b) Case 2: The relative distance between the old target and the new target is a time-varying value

In this case, $\mathbf{P}_e(t)$ is a time-varying value. In order to realise smooth handover of interceptor acceleration, it is required that the velocity derivatives at the beginning time t_0 and the end time $t_0 + T$ of the handover phase exist and are continuous, and the acceleration derivatives exist and are continuous, which is called the second-order smooth handover. Compared with the first-order smooth handover, the phenomenon of excessive acceleration or divergence at the handover time can be avoided.

Therefore, the following expressions need to be satisfied at time t_0 and time $t_0 + T$.

$$\begin{cases} \mathbf{P}_{virtual}(t_0) = \mathbf{P}_{old}(t_0) \\ \dot{\mathbf{P}}_{virtual}(t_0) = \dot{\mathbf{P}}_{old}(t_0) \\ \ddot{\mathbf{P}}_{virtual}(t_0) = \ddot{\mathbf{P}}_{old}(t_0) \\ \dddot{\mathbf{P}}_{virtual}(t_0) = \dddot{\mathbf{P}}_{old}(t_0) \end{cases} \tag{59}$$

$$\begin{cases} \mathbf{P}_{virtual}(t_0 + T) = \mathbf{P}_{old}(t_0 + T) \\ \dot{\mathbf{P}}_{virtual}(t_0 + T) = \dot{\mathbf{P}}_{old}(t_0 + T) \\ \ddot{\mathbf{P}}_{virtual}(t_0 + T) = \ddot{\mathbf{P}}_{old}(t_0 + T) \\ \dddot{\mathbf{P}}_{virtual}(t_0 + T) = \dddot{\mathbf{P}}_{old}(t_0 + T) \end{cases} \tag{60}$$

Meanwhile, according to Equation (54), we take the derivate of $\mathbf{P}_{virtual}(t)$ with respect to time t as

$$\begin{cases} \mathbf{P}_{virtual}(t) = \mathbf{P}_{old}(t) + \lambda(t) \mathbf{P}_e(t) \\ \dot{\mathbf{P}}_{virtual}(t) = \dot{\mathbf{P}}_{old}(t) + \dot{\lambda}(t) \mathbf{P}_e(t) + \lambda(t) \dot{\mathbf{P}}_e(t) \\ \ddot{\mathbf{P}}_{virtual}(t) = \ddot{\mathbf{P}}_{old}(t) + \ddot{\lambda}(t) \mathbf{P}_e(t) + 2\dot{\lambda}(t) \dot{\mathbf{P}}_e(t) + \lambda(t) \ddot{\mathbf{P}}_e(t) \\ \dddot{\mathbf{P}}_{virtual}(t) = \left(\begin{matrix} \dddot{\mathbf{P}}_{old}(t) + \ddot{\lambda}(t) \mathbf{P}_e(t) + 3\dot{\lambda}(t) \dot{\mathbf{P}}_e(t) \\ + 2\dot{\lambda}(t) \ddot{\mathbf{P}}_e(t) + \dot{\lambda}(t) \ddot{\mathbf{P}}_e(t) + \lambda(t) \dddot{\mathbf{P}}_e(t) \end{matrix} \right) \end{cases} \tag{61}$$

At the beginning time t_0 of the handover phase, we can rewrite Equation (61) as

$$\begin{cases} \mathbf{P}_{virtual}(t_0) = \mathbf{P}_{old}(t_0) + \lambda(t_0) \mathbf{P}_e(t_0) \\ \dot{\mathbf{P}}_{virtual}(t_0) = \dot{\mathbf{P}}_{old}(t_0) + \dot{\lambda}(t_0) \mathbf{P}_e(t_0) + \lambda(t_0) \dot{\mathbf{P}}_e(t_0) \\ \ddot{\mathbf{P}}_{virtual}(t_0) = \ddot{\mathbf{P}}_{old}(t_0) + \ddot{\lambda}(t_0) \mathbf{P}_e(t_0) + 2\dot{\lambda}(t_0) \dot{\mathbf{P}}_e(t_0) + \lambda(t_0) \ddot{\mathbf{P}}_e(t_0) \\ \dddot{\mathbf{P}}_{virtual}(t_0) = \left(\begin{matrix} \dddot{\mathbf{P}}_{old}(t_0) + \ddot{\lambda}(t_0) \mathbf{P}_e(t_0) + 3\dot{\lambda}(t_0) \dot{\mathbf{P}}_e(t_0) \\ + 2\dot{\lambda}(t_0) \ddot{\mathbf{P}}_e(t_0) + \dot{\lambda}(t_0) \ddot{\mathbf{P}}_e(t_0) + \lambda(t_0) \dddot{\mathbf{P}}_e(t_0) \end{matrix} \right) \end{cases} \tag{62}$$

According to Equations (59) and (62), we can obtain

$$\begin{cases} \lambda(t_0) = 0 \\ \dot{\lambda}(t_0) = 0 \\ \ddot{\lambda}(t_0) = 0 \\ \dddot{\lambda}(t_0) = 0 \end{cases} \tag{63}$$

At the end time $t_0 + T$ of the handover phase, combining Equation (60), and referring to Equations (61) and (62), we have

$$\begin{cases} \lambda(t_0 + T) = 1 \\ \dot{\lambda}(t_0 + T) = 0 \\ \ddot{\lambda}(t_0 + T) = 0 \\ \dddot{\lambda}(t_0 + T) = 0 \end{cases} \tag{64}$$

Suppose $t_0 = 0$, the time interval of the handover phase $[t_0, t_0 + T]$ is rewritten as $[0, T]$, it is easy to get that

$$\begin{aligned} \lambda(t) = & \eta_1 \sin \frac{\pi}{T}t + \eta_2 \cos \frac{\pi}{T}t + \eta_3 \sin \frac{2\pi}{T}t + \eta_4 \cos \frac{2\pi}{T}t \\ & + \eta_5 \sin \frac{3\pi}{T}t + \eta_6 \cos \frac{3\pi}{T}t + \eta_7 \sin \frac{4\pi}{T}t + \eta_8 \cos \frac{4\pi}{T}t \end{aligned} \tag{65}$$

where $\eta_i (i = 1, 2, \dots, 8)$ are the coefficients of the handover law.

Then, according to Equations (63), (64) and (65), we can obtain

$$\begin{cases} \eta_1 = \eta_3 = \eta_5 = \eta_7 = 0 \\ \eta_2 = -\frac{9}{16}, \eta_4 = \frac{2}{3}, \eta_6 = \frac{1}{16}, \eta_8 = -\frac{1}{6} \end{cases} \tag{66}$$

Therefore, the target handover law can be expressed as

$$\lambda(t) = -\frac{9}{16} \cos \frac{\pi}{T}t + \frac{2}{3} \cos \frac{2\pi}{T}t + \frac{1}{16} \cos \frac{3\pi}{T}t - \frac{1}{6} \cos \frac{4\pi}{T}t \tag{67}$$

Then, substituting Equation (67) into Equation (54), we can obtain

$$\mathbf{P}_{virtual}(t) = \mathbf{P}_{old}(t) + \left(-\frac{9}{16} \cos \frac{\pi}{T}t + \frac{2}{3} \cos \frac{2\pi}{T}t + \frac{1}{16} \cos \frac{3\pi}{T}t - \frac{1}{6} \cos \frac{4\pi}{T}t \right) \mathbf{P}_e(t) \tag{68}$$

According to Equation (68), the virtual target overlaps with the new target at time T , the target changing is achieved.

3.3 Design of whole cooperative midcourse guidance law

3.3.1 Analysis of guidance law in each phase

During combat operations, the constantly changing battlefield situation may necessitate changes in the attack targets. When a target switch occurs, the guidance commands for the interceptors may change abruptly, which needs to be avoided. To address this, we have designed a handover protocol for target information to ensure a smooth transition from the old target information to the new target information, thus preventing sudden changes in guidance commands. During the transition phase of target information, to reduce communication costs and improve accuracy, multiple interceptors will no longer engage in cooperative operations but will independently guide themselves based on the transitional target information. Once the target information update is complete, these interceptors will adjust

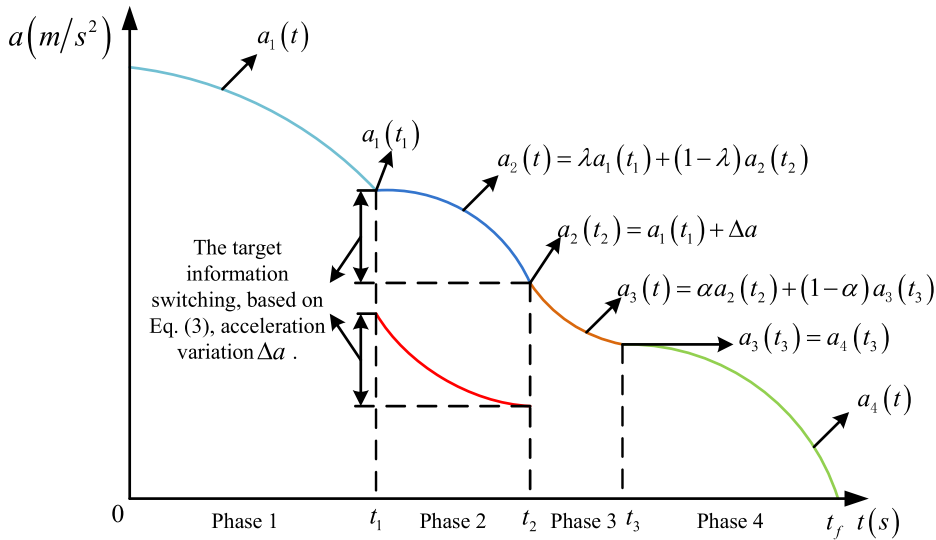


Figure 1. Whole course guidance law.

the network communication topology according to the current battlefield situation, transitioning from single-interceptor guidance to cooperative multi-interceptor attacks on the new target. To avoid abrupt changes in the guidance law, we have also designed a smooth handover protocol from single-interceptor guidance to cooperative multi-interceptor guidance. This design ensures a smooth transition of the guidance law.

Therefore, the design of the guidance law in this paper is mainly divided into four phases, as shown in Fig. 1.

Phase 1 $[0, t_1]$: In this phase, multiple interceptors use the old communication network structure to attack the old target and use guidance law $a_1(t) = a(t)$ for guidance.

Phase 2 $[t_1, t_2]$: This phase is the target changing phase, and there is no coordination between interceptors. In this phase, it is necessary to design the guidance law of the target handover phase. At the beginning time t_1 of the handover phase, the guidance law $a_1(t_1)$ is satisfied, and the guidance law $a_2(t_2)$ is satisfied at the end time t_2 .

Phase 3 $[t_2, t_3]$: In this phase, it is necessary to design the guidance law of the handover phase. At the beginning time t_2 of the handover phase, the guidance law $a_2(t_2)$ is satisfied, and the guidance law $a_3(t_3)$ is satisfied at the end time t_3 .

Phase 4 $[t_3, t_f]$: In this phase, multiple interceptors use the new communication network structure to attack the new target and use guidance law $a_4(t) = a(t)$ for guidance.

3.3.2 Design of guidance law in each phase

(a) Phases 1 and 4 guidance laws

The structures of guidance laws $a_1(t)$ and $a_4(t)$ used in phases 1 and 4 are shown in Equation (21). The communication network structures used in these two phases are different, and the consistency protocol in Equation (21) changes. Because of the target changing or mission change, multiple interceptors need to update the network topology.

(b) Phases 2 and 3 guidance laws

In phases 2 and 3, the guidance laws $a_2(t)$ and $a_3(t)$ of the handover phase need to be designed, and the designed guidance laws meet the requirements of smooth acceleration handover. The guidance

Table 1. Guidance law parameters in handover

time interval	Definition	Guidance law at the beginning	Guidance law at the end	Change rate of guidance law at the beginning of each phase	Change rate of guidance law at the end of each phase
$[t_1, t_2]$		$a_1(t_1)$	$a_2(t_2)$	0	0
$[t_2, t_3]$		$a_2(t_2)$	$a_3(t_3)$	0	0

Table 2. Simulation initial conditions for interceptors

Interceptor	Initial position (x_0, y_0, z_0) (m)	Initial velocity (V_{x0}, V_{y0}, V_{z0}) (m/s)
Interceptor 1	(5, 000, 10, 000, -2, 000)	(1, 150, 50, 60)
Interceptor 2	(3, 000, 9, 500, 1, 000)	(1, 200, 20, 50)
Interceptor 3	(1, 500, 8, 500, -1, 000)	(1, 250, 30, 50)
Interceptor 4	(2, 500, 9, 000, -1, 500)	(1, 250, 30, 50)

laws are designed by Hermite interpolation. This method requires that the interpolation function and the interpolated function have equal function values at the node x_i , equal derivative values, and equal higher-order derivatives.

The guidance law parameters for the handover phase are shown in Table 1.

Substituting the data in Table 1 into Equation (20), and by Lemma 4, the handover guidance law of phase 2 is designed as

$$a_2(t) = \left(1 + 2\frac{t-t_1}{T_1}\right) \left(\frac{t-t_2}{-T_1}\right)^2 a_1(t_1) + \left(1 + 2\frac{t-t_2}{T_1}\right) \left(\frac{t-t_1}{T_1}\right)^2 a_2(t_2) \tag{69}$$

where, $T_1 = t_2 - t_1$ denotes the target handover time of phase 2; $a_1(t_1)$ is the size of the guidance law designed in Section (a) at time t_1 ; $a_2(t_2)$ can be expressed as

$$a_2(t_2) = a_1(t_1) + \Delta a \tag{70}$$

where $\Delta a = a_0(t_2) - a_0(t_1)$ is the acceleration variation of the trajectory shaping guidance law in phase 2.

Referring to phase 2, the handover guidance law of phase 3 is designed similarly as

$$a_3(t) = \left(1 + 2\frac{t-t_2}{T_2}\right) \left(\frac{t-t_3}{-T_2}\right)^2 a_2(t_2) + \left(1 + 2\frac{t-t_3}{T_2}\right) \left(\frac{t-t_2}{T_2}\right)^2 a_3(t_3) \tag{71}$$

where, $T_2 = t_3 - t_2$ is the target handover time of phase 3; $a_3(t_3)$ indicates the size of the guidance law designed in Section (a) at time t_3 for the interceptor in the new network topology.

4.0 Simulation and analysis

In order to verify the effectiveness and performance of the cooperative midcourse guidance law with target changing and topology switching in the case of target loss and communication topology switching of multiple interceptors intercepting targets, the numerical examples are provided in this section.

In the simulation, four interceptors are selected for cooperative interception verification. The parameters of four interceptors are shown in Table 2.

Table 3. Parameters of the old target

Initial position (x_0, y_0, z_0) (m)	Initial velocity (V_{x0}, V_{y0}, V_{z0}) (m/s)
(85, 000, 8, 000, 0)	(280, 0, 0)

Table 4. Parameters of the new target

Initial position (x_0, y_0, z_0) (m)	Initial velocity (V_{x0}, V_{y0}, V_{z0}) (m/s)
(90, 000, 15, 000, 0)	(280, 0, 0)

In phase 1, four interceptors intercept the old target cooperatively. In phase 2, according to the mission requirements, the fourth interceptor intercepts the old target, and the remaining three interceptors intercept the new target. The parameters of cooperative guidance law are selected as $\alpha_{xi} = \alpha_{yi} = \alpha_{zi} = 0.01$ and $\alpha_{xij} = \alpha_{yij} = \alpha_{zij} = 1$. At the end of the midcourse guidance phase, the elevation angle of LOS and the azimuth angle of LOS constraints of all interceptors are selected as $q_e = q_\beta = 20^\circ$. The midcourse and terminal handover distance is set 10km. The target handover time is selected as $t = 10$ s. According to Equation (52), the maximum allowable heading error is selected as $\Delta\gamma_{\max} = 15^\circ$, we have $T \leq 20.94$ s. Therefore, the phase 2 time is selected as $T_1 = 20$ s and the phase 3 time is selected as $T_2 = 10$ s.

Before switching the target, the old network communication topology is selected as

$$A = \begin{bmatrix} 0 & 1 & 1 & 0 \\ 1 & 0 & 0 & 1 \\ 1 & 0 & 0 & 1 \\ 0 & 1 & 1 & 0 \end{bmatrix}$$

After switching the target, the new network communication topology is selected as

$$A = \begin{bmatrix} 0 & 1 & 1 \\ 1 & 0 & 0 \\ 1 & 0 & 0 \end{bmatrix}$$

4.1 Case 1: The relative distance between the old target and the new target is a constant value

The old target parameters are shown in Table 3.

The new target parameters are shown in Table 4.

The relative distance between the new target and the old target is shown in Fig. 2. It can be seen from Fig. 2 that the relative distance between the old target and the new target is always a constant value.

The trajectories of multiple interceptors under the cooperative guidance law Equation (21) and the guidance law Equation (3) are shown in Fig. 3. It can be seen from Fig. 3 that in the initial stage of flight, the trajectories of the four interceptors all point to the old target. When the target changes, the trajectories of interceptors 1, 2 and 3 change significantly, all pointing to the new target. The interceptor 4 still attacks the old target, and it is obvious that its trajectory direction has not changed.

The relative distances between interceptors and targets and the times-to-go of interceptors are shown in Figs. 4–5. It can be seen from Figs. 4–5 that in phase 2 T_1 and phase 3 T_2 , the relative distance and the times-to-go of interceptors 1, 2 and 3 with target change are obviously different from those of interceptor 4 without target change. When the target change is completed, the relative distances of the interceptors 1, 2, 3 can still reach the constraint range of the midcourse and terminal handover at the same time according to the designed cooperative guidance law, and the times-to-go can reach the same.

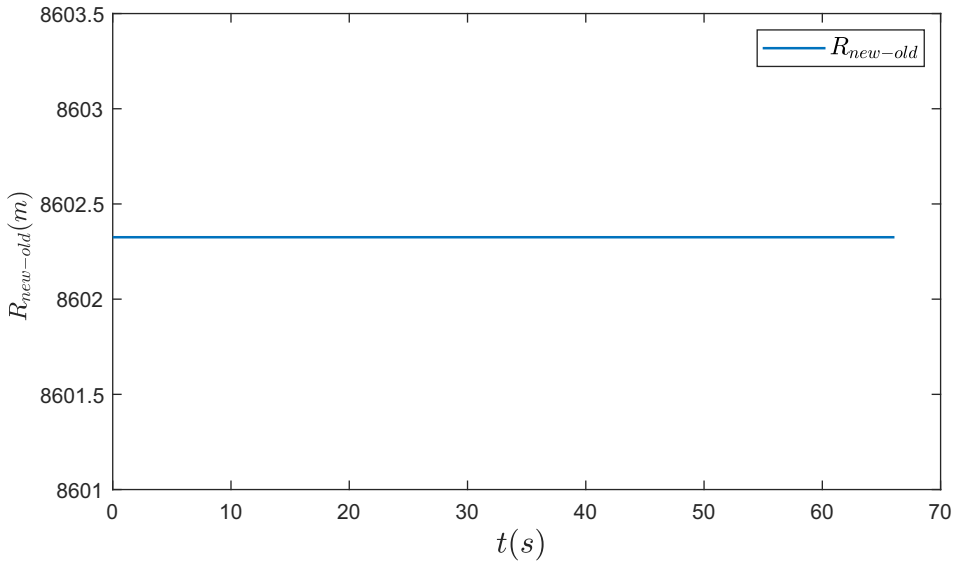


Figure 2. The relative distance between the new target and the old target.

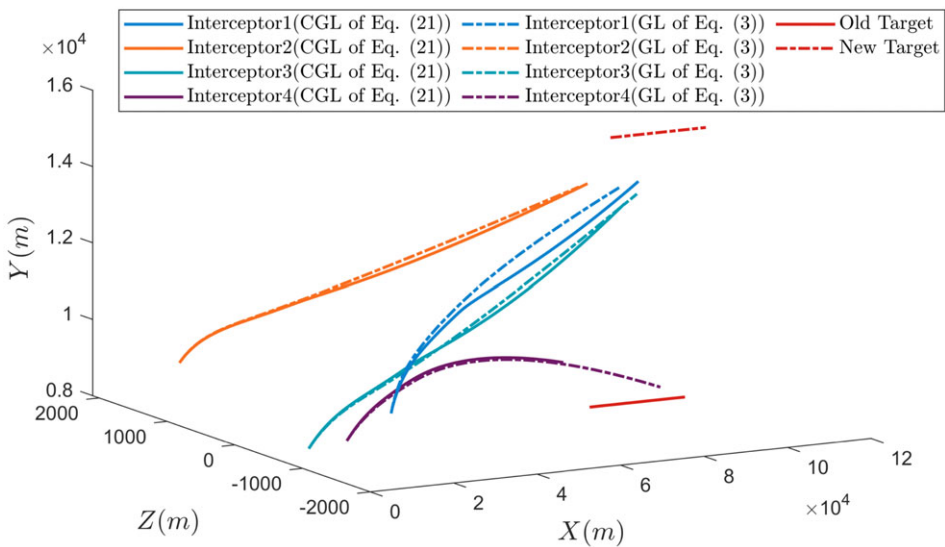


Figure 3. The trajectories of interceptors and targets.

However, it is evident that under the guidance law Equation (3), the relative distances and times-to-go of all interceptors cannot converge, making cooperation unattainable.

The accelerations of interceptors 1, 2, 3, 4 are shown in Figs. 6–9, respectively. It can be seen from Figs. 6–9 that the accelerations of the interceptors 1, 2, 3 change significantly, and the smooth handover can be achieved in phase 2 T_1 and phase 3 T_2 without abrupt change. The acceleration of interceptor 4 only achieves a smooth handover in phase 2 T_1 . Because the guidance command of interceptor 4 is the handover from the cooperative guidance command of four interceptors designed at the beginning to the guidance command of a single interceptor. Subsequent flight interceptor 4 does not need to cooperate with the other three interceptors, so interceptor 4 does not have the handover time of phase 3 T_2 .

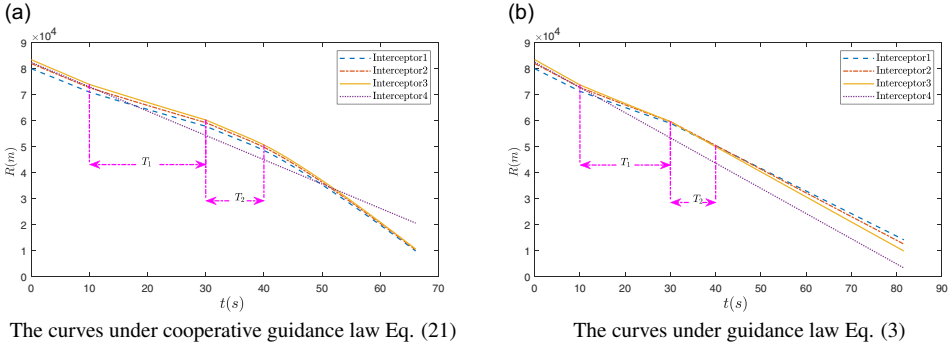


Figure 4. The relative distances between interceptors and targets.

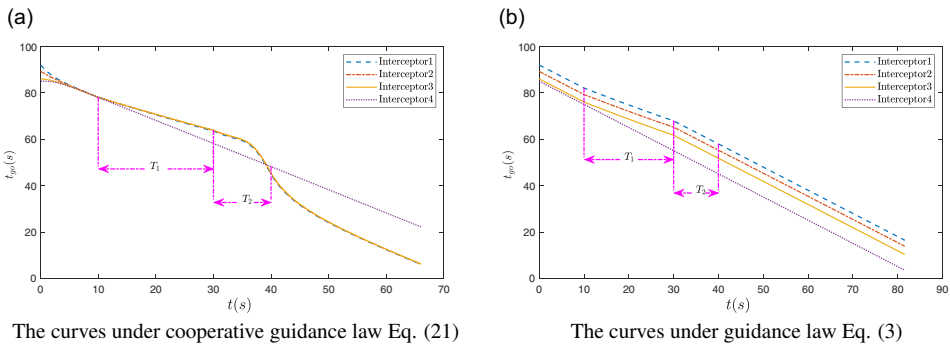


Figure 5. The times-to-go of interceptors.

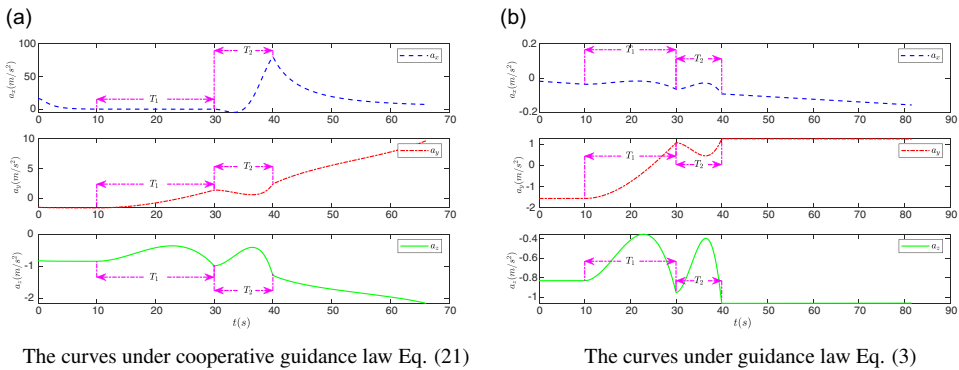
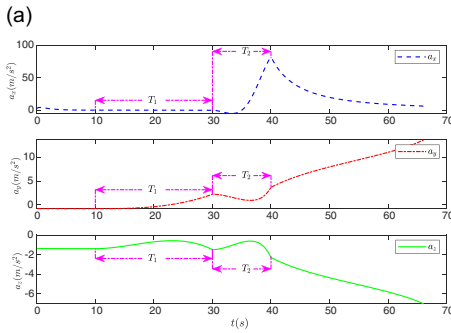


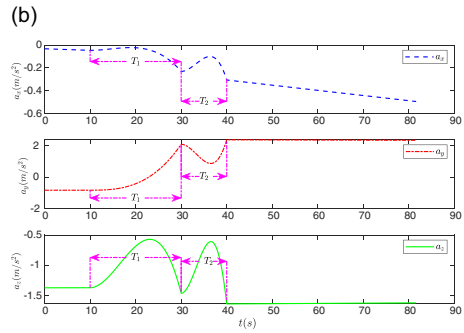
Figure 6. The accelerations of interceptor 1.

It is evident that the acceleration designed according to Equation (3) is much smaller than the acceleration designed according to Equation (21). This is mainly because if the interceptors aim to achieve cooperation, the cooperation term $\alpha_{xi}(\hat{P}_{xi}(t) - \hat{P}_x(t))$ must play a major role, thereby making the state quantities of all interceptors converge in each direction to achieve cooperation.

The elevation angles and the azimuth angles of the LOS and the velocities of the four interceptors are shown in Figs. 10–12, respectively. It can be seen from Figs. 10–12 that the elevation angles, azimuth angles of the LOS, and the velocities of the four interceptors can reach the constraint range for midcourse

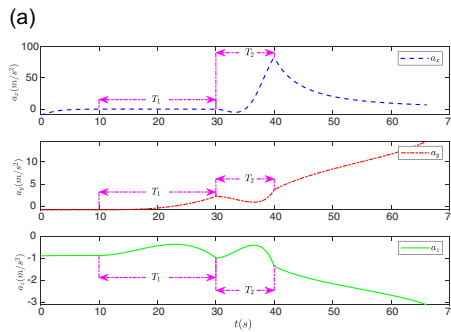


The curves under cooperative guidance law Eq. (21)

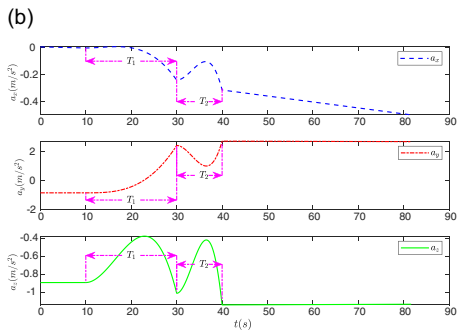


The curves under guidance law Eq. (3)

Figure 7. The accelerations of interceptor 2.

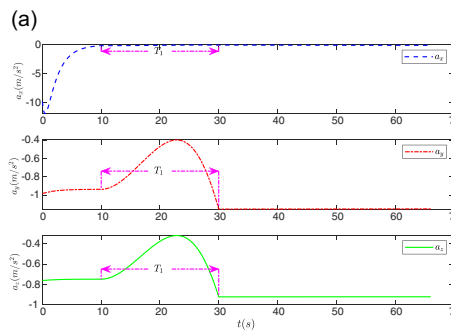


The curves under cooperative guidance law Eq. (21)

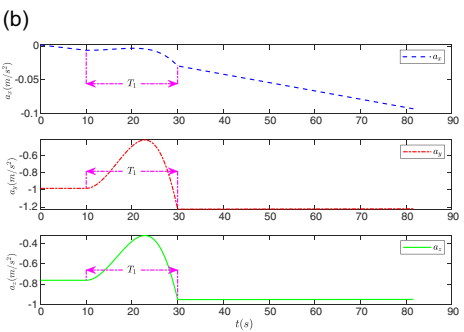


The curves under guidance law Eq. (3)

Figure 8. The accelerations of interceptor 3.



The curves under cooperative guidance law Eq. (21)



The curves under guidance law Eq. (3)

Figure 9. The accelerations of interceptor 4.

and terminal handover. When the target changes, the elevation angles and azimuth angles of the LOS and the velocities of interceptors 1, 2, and 3 do not change abruptly during phase 2 T_1 and phase 3 T_2 . The elevation angle, azimuth angle of the LOS, and velocity of interceptor 4 do not change abruptly in phase 2 T_1 .

It can be seen that under the guidance law Equation (21), the speed of the interceptors increases significantly, reducing the relative distances and the differences in the times-to-go between the interceptors,

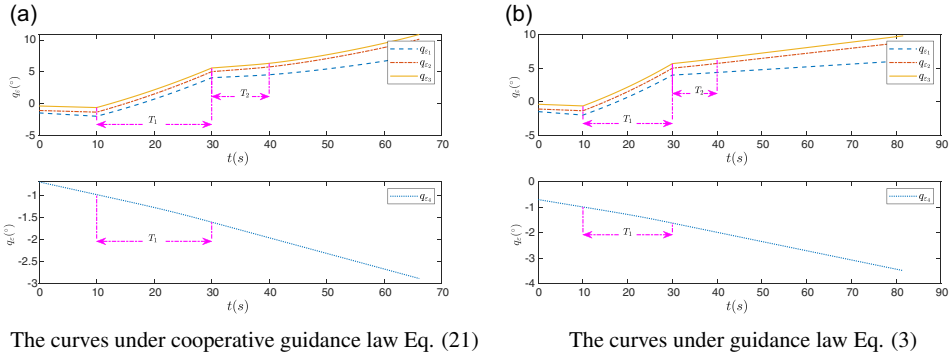


Figure 10. The elevation angles of LOS.

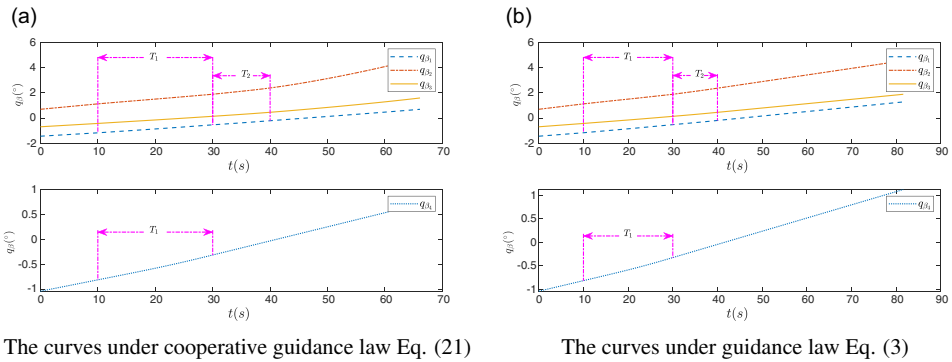


Figure 11. The azimuth angles of LOS.

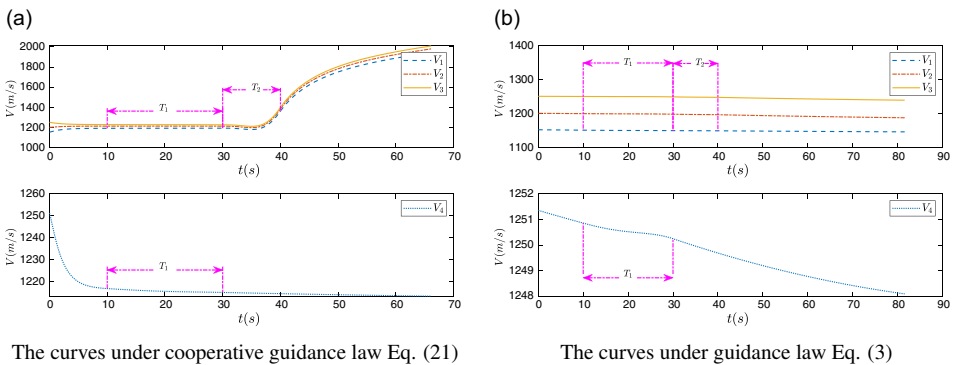


Figure 12. The velocities of interceptors.

thereby achieving cooperation. Under the guidance law Equation (3), there is no significant difference in the speed of the interceptors, and thus the relative distances and differences in the times-to-go between the interceptors cannot be reduced, resulting in a failure to achieve cooperation.

Obviously, when the interceptors change target, the proposed guidance law can achieve satisfactory performance. The simulation results show that the accelerations achieve a smooth handover without

Table 5. Parameters of the old target

Initial position (x_0, y_0, z_0) (m)	Initial velocity (V_{x0}, V_{y0}, V_{z0}) (m/s)
(85, 000, 8, 000, 0)	(280, 0, 0)

Table 6. Parameters of the new target

Initial position (x_0, y_0, z_0) (m)	Initial velocity (V_{x0}, V_{y0}, V_{z0}) (m/s)
(95, 000, 10, 000, 2, 000)	(300, 10, 10)

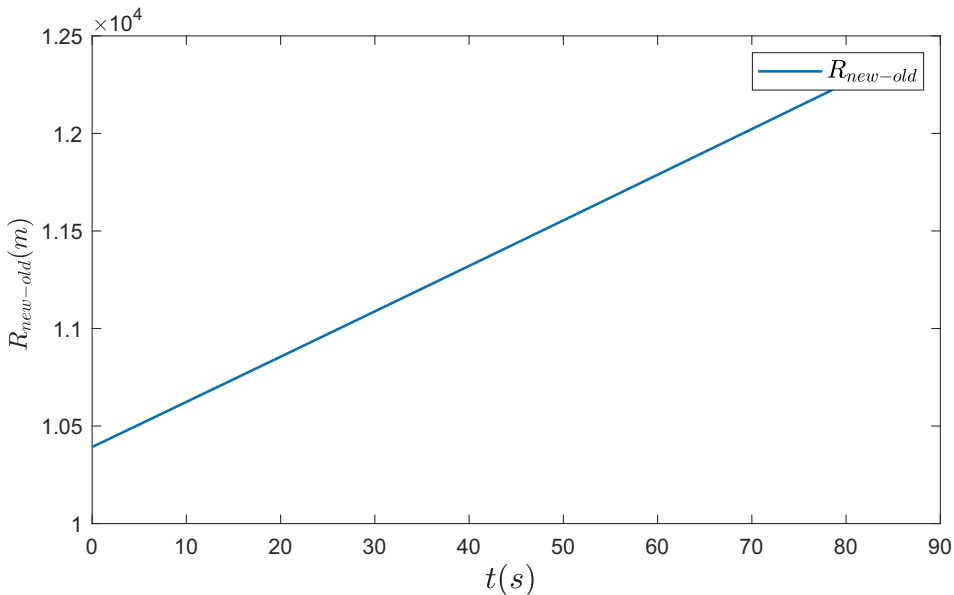


Figure 13. The relative distance between the new target and the old target.

abrupt change in phases 2 and 3. The designed guidance law can ensure that each interceptor completes the midcourse guidance mission and meets the midcourse and terminal handover constraints.

4.2 Case 2: The relative distance between the old target and the new target is a time-varying value

The old target parameters are shown in Table 5.

The new target parameters are shown in Table 6.

The relative distance between the new target and the old target is shown in Fig. 13. It can be seen from Fig. 13 that the relative distance between the old target and the new target varies linearly.

The trajectories of multiple interceptors under the cooperative guidance law Equation (21) and the guidance law Equation (3) are shown in Fig. 14. It can be seen from Fig. 14 that in the initial stage of flight, the trajectories of the four interceptors all point to the old target. When the target changes, the trajectories of interceptors 1, 2 and 3 change significantly, all pointing to the new target. The interceptor 4 still attacks the old target, and it is obvious that its trajectory direction has not changed.

The relative distances between interceptors and targets and the times-to-go of interceptors are shown in Figs. 15–16. It can be seen from Figs. 15–16 that in phase 2 T_1 and phase 3 T_2 , the relative distance

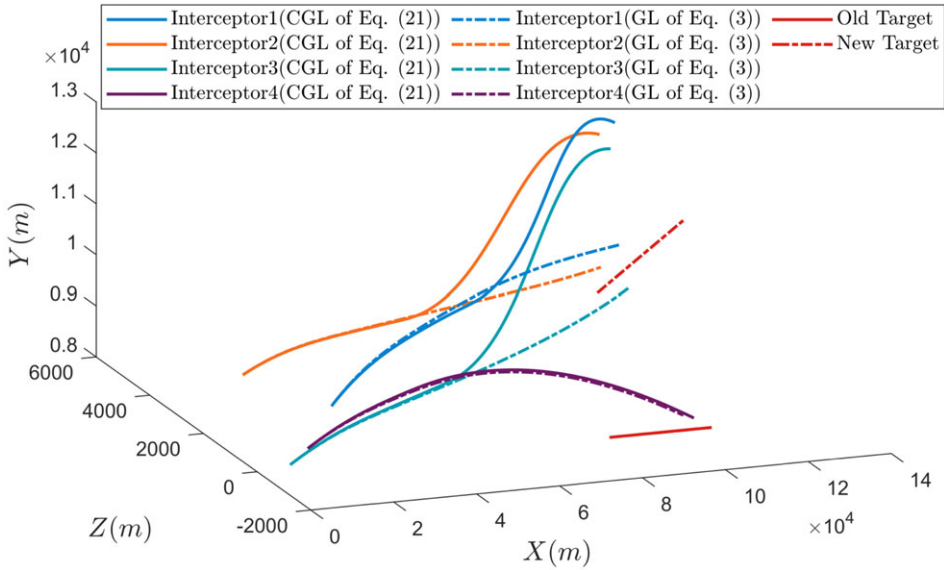


Figure 14. The trajectories of interceptors and targets.

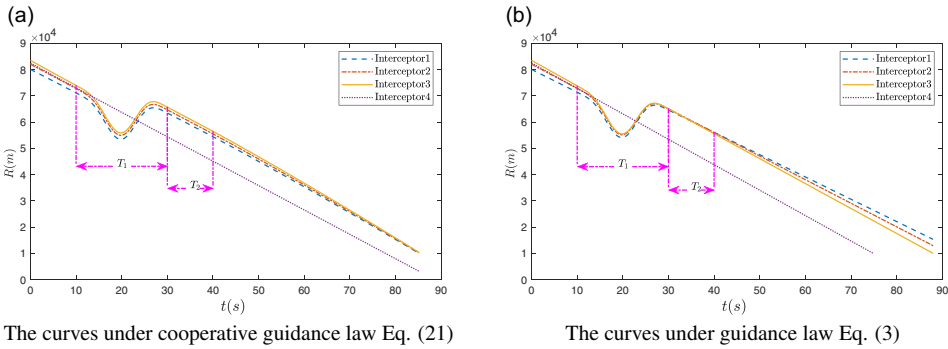


Figure 15. The relative distances between interceptors and targets.

and the times-to-go of interceptors 1, 2 and 3 with target change are obviously different from those of interceptor 4 without target change. When the target change is completed, the relative distances of the interceptors 1,2,3 can still reach the constraint range of the midcourse and terminal handover at the same time according to the designed cooperative guidance law, and the times-to-go can reach the same. However, it is evident that under the guidance law Equation (3), the relative distances and times-to-go of all interceptors cannot converge, making cooperation unattainable.

The accelerations of interceptors 1, 2, 3, 4 are shown in Figs. 17–20, respectively. It can be seen from Figs. 17–20 that the accelerations of the interceptors 1, 2, 3 change significantly, and the smooth handover can be achieved in phase 2 T_1 and phase 3 T_2 without abrupt change. The acceleration of interceptor 4 only achieves a smooth handover in phase 2 T_1 . Because the guidance command of interceptor 4 is the handover from the cooperative guidance command of four interceptors designed at the beginning to the guidance command of a single interceptor. Subsequent flight interceptor 4 does not need to cooperate with the other three interceptors, so interceptor 4 does not have the handover time of phase 3 T_2 . It is evident that the acceleration designed according to Equation (3) is much smaller than the acceleration designed according to Equation (21). This is mainly because if the interceptors aim to

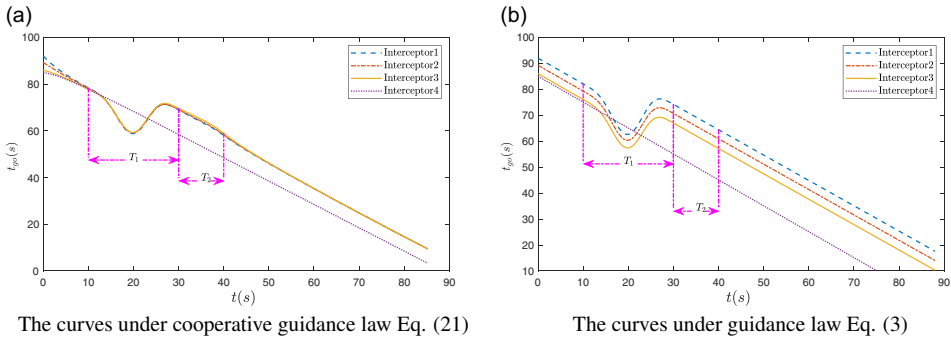


Figure 16. The times-to-go of interceptors.

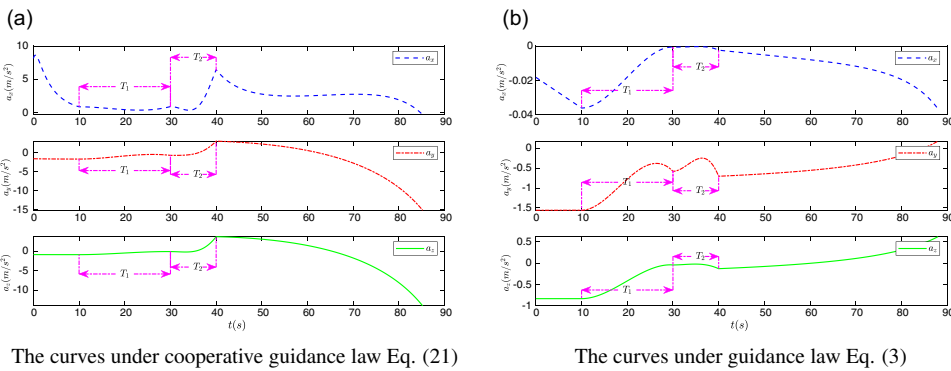


Figure 17. The accelerations of interceptor 1.

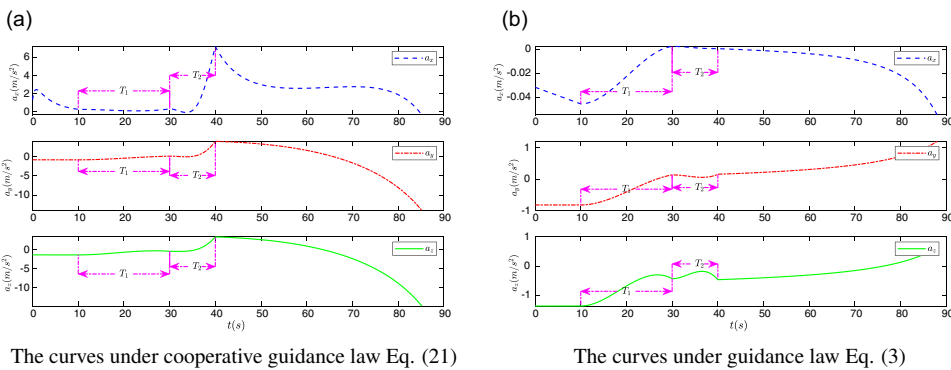
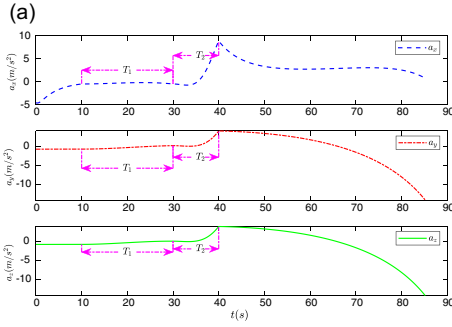


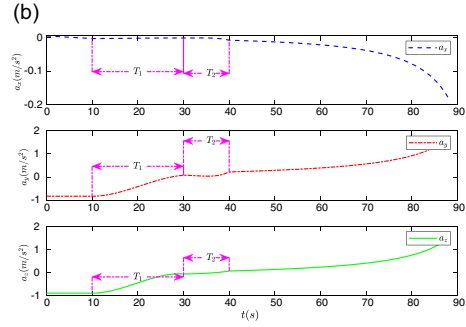
Figure 18. The accelerations of interceptor 2.

achieve cooperation, the cooperation term $\alpha_{xi}(\hat{P}_{xi}(t) - \hat{P}_x(t))$ must play a major role, thereby making the state quantities of all interceptors converge in each direction to achieve cooperation.

The elevation angles and the azimuth angles of the LOS and the velocities of the four interceptors are shown in Figs. 21–23, respectively. It can be seen from Figs. 21–23 that the elevation angles, azimuth angles of the LOS, and the velocities of the four interceptors can reach the constraint range for midcourse and terminal handover. When the target changes, the elevation angles and azimuth angles of the LOS

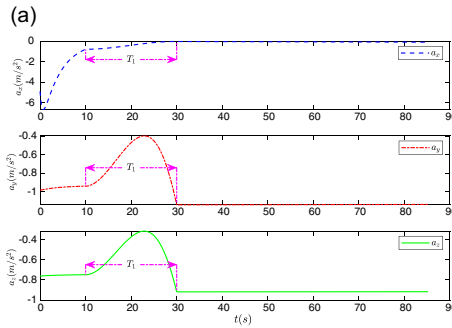


The curves under cooperative guidance law Eq. (21)

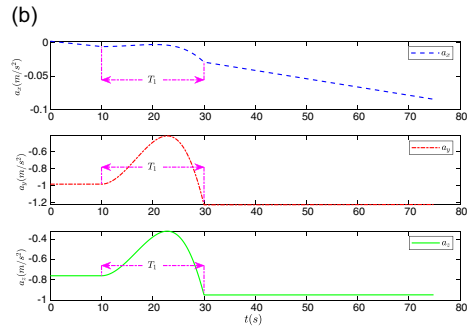


The curves under guidance law Eq. (3)

Figure 19. The accelerations of interceptor 3.

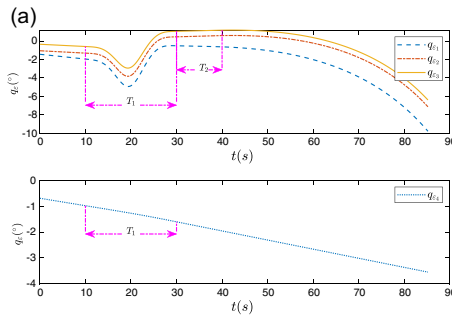


The curves under cooperative guidance law Eq. (21)

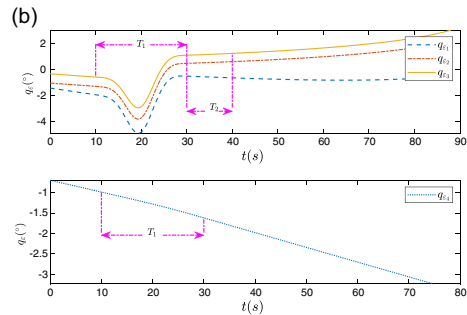


The curves under guidance law Eq. (3)

Figure 20. The accelerations of interceptor 4.



The curves under cooperative guidance law Eq. (21)



The curves under guidance law Eq. (3)

Figure 21. The elevation angles of LOS.

and the velocities of interceptors 1, 2, and 3 do not change abruptly during phase 2 T_1 and phase 3 T_2 . The elevation angle, azimuth angle of the LOS, and velocity of interceptor 4 do not change abruptly in phase 2 T_1 .

It can be seen that under the guidance law Equation (21), the speed of the interceptors increases significantly, reducing the relative distances and the differences in the times-to-go between the interceptors, thereby achieving cooperation. Under the guidance law Equation (3), there is no significant difference in

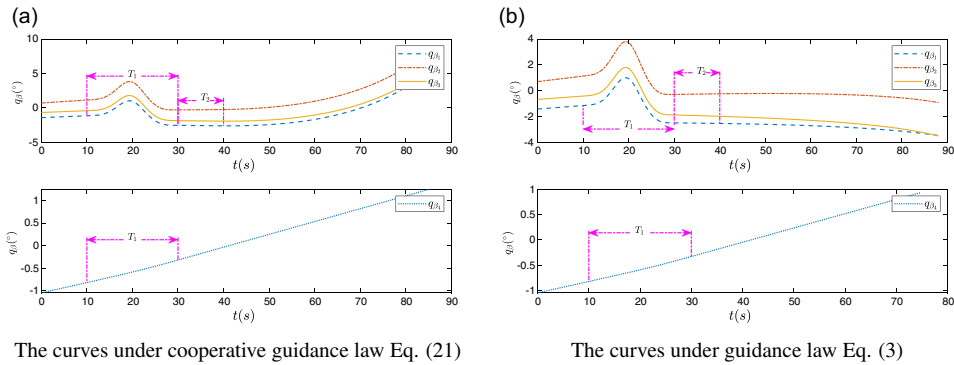


Figure 22. The azimuth angles of LOS.

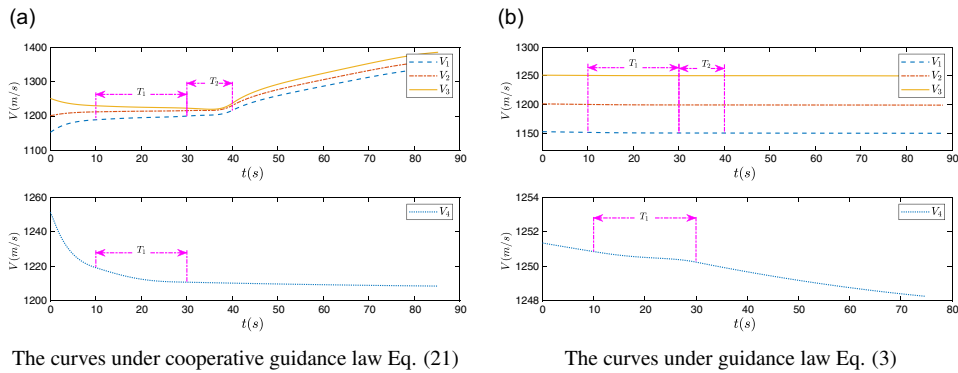


Figure 23. The velocities of interceptors.

the speed of the interceptors, and thus the relative distances and differences in the times-to-go between the interceptors cannot be reduced, resulting in a failure to achieve cooperation.

The simulation results show that in case 2, the cooperative guidance law method can still ensure smooth acceleration handover for each interceptor, successfully complete the midcourse guidance mission, and meet the midcourse and terminal handover constraints.

The above simulation results demonstrate that, under the guidance law Equation (21) designed in this paper, multiple interceptors can achieve cooperative flight to the midcourse and terminal handover area. Furthermore, a comparison with the simulation results of interceptors under guidance law Equation (3) verifies the superiority of the guidance method designed in this paper.

5.0 Conclusion

In this paper, the cooperative midcourse guidance law method with target changing and topology switching has been proposed for distributed interceptor clusters. The average position consistency protocol of virtual interception points has been designed based on cooperative trajectory shaping guidance law. Then, the convergence of the cooperative states in the guidance system has been proved by Lyapunov stability theory, and the cooperative interception mission under the condition of communication topology switching has been completed. Furthermore, based on the acceleration smoothing theory, the target handover law and the handover guidance law have been designed to realise the smooth handover between

each phase. The numerical simulation results show that when the interceptor changes the target, the proposed guidance law method can ensure the smooth handover of acceleration and meet the constraints of midcourse and terminal handover, and further show the effectiveness and superiority of the proposed method.

For future research, a more in-depth analysis will be conducted regarding the differences between coordinated (organised but non-reactive) and cooperative (organised and reactive to environmental changes) interceptor formations.

Data availability statement. The data used to support the findings of this study are included within the article.

Competing interests. The authors declared that they have no conflicts of interest to this work.

Acknowledgements. The authors would like to thank the associate editor and reviewers for their valuable comments and constructive suggestions that helped to improve the paper and presentation significantly.

References

- [1] Jeon, I.S., Lee, J.I. and Tank, M.J. Impact-time-control guidance law for anti-ship missiles, *IEEE Trans. Control Syst. Technol.*, 2006, **14**, (2), pp 260–266.
- [2] Xu, C. and Lv, T. Cooperative guidance law for multiple UAVs impact times consensus in finite time, *Tactical Missile Technol.*, 2020, (6), pp 44–56.
- [3] Zhang, Y., Tang, S. and Guo, J. Two-stage cooperative guidance strategy using a prescribed-time optimal consensus method, *Aerospace Sci. Technol.*, 2020, **100**, p 105641.
- [4] Yang, X. and Song, S. Three-dimensional consensus algorithm for nonsingular distributed cooperative guidance strategy, *Aerospace Sci. Technol.*, 2021, **118**, p 106958.
- [5] Zhai, J. and Yang, J. An event-triggered distributed cooperative guidance law for simultaneous attack with autopilot lag consideration, *Trans. Inst. Meas. Control.*, 2023, **45**, (11), pp 2043–2058.
- [6] Chen, Y., Liu, J., Shan, J. and Wang, J. Impact angle, speed and acceleration control guidance via polynomial trajectory shaping, *J. Franklin Inst.-Eng. Appl. Math.*, 2023, **360**, (7), pp 4923–4946.
- [7] Song, J., Song, S. and Xu, S. Three-dimensional cooperative guidance law for multiple missiles with finite-time convergence, *Aerospace Sci. Technol.*, 2017, **67**, (8), pp 193–205.
- [8] Kumar, S.R. and Mukherjee, D. Terminal time-constrained nonlinear interception strategies against maneuvering targets, *J. Guid. Control Dyn.*, 2021, **44**, (1), pp 200–209.
- [9] Ma, M. and Song, S. Multi-missile cooperative guidance law for intercepting maneuvering target, *Aero Weaponry*, 2021, **28**, (6), pp 19–27.
- [10] Li, H., Liu, Y., Li, K. and Liang, Y. Polynomial guidance for impact-time control against maneuvering targets, *J. Guid. Control Dyn.*, 2023, **46**, (12), pp 2388–2398.
- [11] You, H., Chang, X., Zhao, J., Wang, S. and Zhang, Y. Three-dimensional impact-angle-constrained cooperative guidance strategy against maneuvering target, *ISA Trans.*, 2023, **138**, pp 262–280.
- [12] Tao, H., Lin, D., Song, T. and Li, H. Optimal spatial-temporal cooperative guidance against a maneuvering target, *J. Franklin Inst.-Eng. Appl. Math.*, 2023, **360**, (13), pp 9886–9903.
- [13] Zhang, Z., Dong, X., Yv, J., Li, Q. and Ren, Z. Distributed cooperative tracking and cooperative guidance against maneuvering aerial target, *Aerospace Sci. Technol.*, 2024, **144**, p 108827.
- [14] Sun, X., Hou, D., Zhou, R. and Wu, J. Consensus of leader-followers system of multi-missile with time-delays and switching topologies, *Optik*, 2014, **125**, (3), pp 1202–1208.
- [15] Ning, B., Jin, J. and Zheng, J. Fixed-time consensus for multi-agent systems with discontinuous inherent dynamics over switching topology, *Int. J. Syst. Sci.*, 2017, **48**, (9), pp 2023–2032.
- [16] Zhao, Q., Dong, X., Song, X. and Ren, Z. Cooperative time-varying formation guidance for leader-following missiles to intercept a maneuvering target with switching topologies, *Nonlinear Dynamics*, 2019, **95**, (1), pp 129–141.
- [17] Zhao, E., Yang, M., Chao, T. and Wang, S. Cooperative interception for multiple flight vehicles with switching topologies, *J. Astronaut.*, 2019, **40**, (6), pp 646–654.
- [18] Sun, M., Ren, L., Liu, J. and Sun, C. Dynamic event-triggered fixed-time average consensus control of multi-agent systems under switching topologies, *Acta Automat. Sinica*, 2022, **48**, (4), pp 1–11.
- [19] Shin, H.S., Tsourdos, A., Méneç, S., Markham, K. and White, B. Cooperative mid course guidance for area air defence, AIAA Guidance, Navigation, Control Conference, 2013.
- [20] Kumar, S.R., Tsalik, R. and Shima, T. Nonlinear robust inscribed angle guidance for stationary targets, *J. Guid. Control Dyn.*, 2017, **40**, (7), pp 1815–1823.
- [21] Wang, L., Yao, Y., He, F. and Liu, K. A novel cooperative mid-course guidance scheme for multiple intercepting missiles, *Chin. J. Aeronaut.*, 2017, **30**, (3), pp 1140–1153.
- [22] Zhang, H., Tang, S. and Guo, J. Cooperative near-space interceptor mid-course guidance law with terminal handover constraints, *Proc. Inst. Mech. Eng. Part G J. Aerospace Eng.*, 2019, **233**, (6), pp 1960–1976.

- [23] Wu, Z., Fang, Y., Fu, W., Wang, Z. and Ma, W. Three-dimensional cooperative mid-course guidance law against the maneuvering target, *IEEE Access.*, 2020, **8**, (99), pp 18841–18851.
- [24] Wu, Z., Ren, Q., Luo, Z., Fang, Y. and Fu, W. Cooperative midcourse guidance law with communication delay, *Int. J. Aerospace Eng.*, 2021, **2021**, (1), p 3460389.
- [25] Hou, M., Liu, H. and Zhang, J. Handover rule of combined guidance for medium and long range tactical missiles, *Electro-optic Control*, 1998, **4**, pp 4–20.
- [26] Wang, G. Research on compound guidance of long-range air-to-air missile (Thesis), Northwestern Polytechnical University, 2004.
- [27] Li, Z., Song, Z. and Chen, Y. A strategy of midcourse and terminal guidance handover in combined guidance, *J. Mod. Def. Technol.*, 2011, **39**, (3), pp 74–77.
- [28] Zhang, L., Fang, Y., Gao, X. and Diao, X. Study on trajectory shifted law of midcourse and terminal guidance handover. *Journal of Ballistics.*, 2014, **26**, (2), pp 12–16.
- [29] Liu, X., Lv, M., Zhang, K., Duan, M. and Yang, T. Research on trajectory shifted law of midcourse and terminal guidance handover based on 2-order smooth condition, Proceedings of the 34th Chinese Control Conference.
- [30] Li, C., Wang, J., Li, B., He, S. and Zhang, T. Energy-optimal guidance law with virtual hand-over point, *Acta Aeronaut. Astronaut. Sinica.*, 2019, **40**, (12), pp 10–25.
- [31] Liu, J., Chen, S., Chen, Y., Duan, C. and Liu, M. A midcourse and terminal trajectory handover method suitable for composite guidance missiles, *Tactical Missile Technol.*, 2020, (2), pp 7–15.
- [32] Lukacs, J. and Yakimenko, O. Trajectory-shape-varying missile guidance for interception of ballistic missiles during the boost phase, AIAA Guidance, Navigation and Control Conference and Exhibit, 2007.
- [33] Hong, Y., Xu, Y. and Jie, H. Finite-time control for robot manipulators, *Syst. Control Lett.*, 2002, **46**,(4), pp 243–253.
- [34] Bhat, S.P. and Bernstein, D.S. Finite-time stability of continuous autonomous systems, *SIAM J.Control Optim.*, 2000, **38**, (3), pp 751–766.
- [35] Long, W. and Feng, X. Finite-time consensus problems for networks of dynamic agents, *IEEE Trans. Autom. Control*, 2010, **55**, (4), pp 950–955.
- [36] Zhang, H. Research on defense guidance technology of hypersonic cruise target (Thesis), Beijing Institute of Technology, 2018.